

## A new diverse enantiornithine family (Bohaiornithidae fam. nov.) from the Lower Cretaceous of China with information from two new species

WANG Min<sup>1,2</sup> ZHOU Zhong-He<sup>1</sup> Jingmai K. O'CONNOR<sup>1</sup> Nikita V. ZELENKOV<sup>3</sup>

(1 Key Laboratory of Vertebrate Evolution and Human Origins of Chinese Academy of Sciences, Institute of Vertebrate Paleontology and Paleoanthropology, Chinese Academy of Sciences Beijing 100044 wangmin@ivpp.ac.cn)

(2 University of Chinese Academy of Sciences Beijing 100049)

(3 Borissiak Palaeontological Institute of the Russian Academy of Sciences Moscow 117997)

**Abstract** Two new enantiornithine birds, *Parabohaiornis martini* gen. et sp. nov., and *Longusunguis kurochkini* gen. et sp. nov., are reported here based on three nearly complete skeletons from the Lower Cretaceous lacustrine deposits of the Jiufotang Formation in Liaoning, northeastern China. The two new species share several unique features with *Bohaiornis*, *Shenqiornis*, *Sulcavis* and *Zhouornis*, including a robust rostrum with robust, subconical teeth, furcula with blunt omal expansions, sternal trabeculae caudolaterally directed, short and stout tarsometatarsus with hypertrophied ungual on digit III. A close relationship among the two new species and four previously described taxa is confirmed by a comprehensive phylogenetic analysis, leading us to erect Bohaiornithidae fam. nov. With six known taxa, Bohaiornithidae is the most diverse recognized enantiornithine family. The robust morphology of the rostrum and foot suggests bohaiornithids occupied a specialized ecological niche compared to other Early Cretaceous enantiornithines.

**Key words** Early Cretaceous, Jehol Biota, Enantiornithes, *Bohaiornis*, *Shenqiornis*, *Sulcavis*, *Zhouornis*

### 1 Introduction

The abundant and continuous discoveries of exquisitely preserved plant, invertebrate, and vertebrate fossils from the Lower Cretaceous of China have made the Jehol Biota one of the world's most important Mesozoic terrestrial biomes (Chang et al., 2001; Zhou et al., 2003; Zhou, 2006). Over the last three decades, hundreds of non-avian dinosaur and bird specimens have been discovered in the Jehol Group, providing extraordinary information addressing issues such as the origin and evolution of feathers and flight, the origin of birds, and the morphology and ecology of basal birds and their non-avian theropod relatives (Xu et al., 2001,

---

国家重点基础研究发展计划(973)项目(编号: 2012CB821906)和国家自然科学基金创新研究群体科学基金(批准号: 41172020)资助。

收稿日期: 2013-07-26

2009, 2010, 2011; Zhou and Zhang, 2003a, 2006a; Zhou, 2004; Chiappe, 2007; O'Connor et al., 2011a). Enantiornithes are the dominant avian clade within the Jehol Biota in terms of taxonomic diversity; nearly 27 enantiornithine birds have been named and the rate of discovery continues to be high (Zhou and Hou, 2002; Zhou and Zhang, 2006a; Wang et al., in press a,b). Due to the blooming discoveries and simultaneous publications of similar specimens, comparisons between known taxa have often been limited, resulting in many poorly diagnosed taxa of uncertain validity, and higher level relationships are all but unknown (O'Connor and Dyke, 2010). Only a limited amount of taxonomic revision has been conducted, leaving numerous issues unresolved (e.g., naming taxa on fragmentary fossils)(O'Connor, 2009, 2012; O'Connor and Dyke, 2010; O'Connor et al., 2009, 2011b).

Recently, Hu et al. (2011) described a large enantiornithine bird, *Bohaiornis guoi*, from the Early Cretaceous deposits near the Lamadong Town, Jianchang Country, northeastern China. The fossil was from the Jiufotang Formation rather than the Yixian Formation stated by Hu et al. (2011), because the Yixian Formation is largely unexposed in this area (He et al., 2004; Wang X L personal communication). The holotype LPM B00167 is largely complete but the poor condition of the fossil preservation obscures details in the skull, vertebrae, pelvis and hindlimbs. The new taxon was included in a phylogenetic analysis performed on a relatively old data matrix including only 18 taxa and 54 characters, and thus the results were not informative except in that they confirmed the enantiornithine affinity of *Bohaiornis* (Hu et al., 2011). More recently, Li et al. (in press) described a referred specimen of *Bohaiornis* (IVPP V 17963), providing new morphological information and an amended diagnosis for the genus. *Bohaiornis* bears a strong similarity to several recently described taxa, including *Shenqiornis* Wang et al., 2010, the recently reported *Sulcavis* O'Connor et al., 2013, and *Zhouornis* Zhang et al., 2013, but these taxa have never been comprehensively compared to one another.

Here we describe three new enantiornithine specimens, all collected from localities near those that produced *Bohaiornis* and *Sulcavis*; whereas, *Shenqiornis* was from the Qiaotou Formation in Hebei Province, and the provenance of *Zhouornis* needs to be confirmed (Wang et al., 2010; O'Connor et al., 2013; Zhang et al., 2013; Li et al., in press). The new specimens resemble *Bohaiornis*, *Shenqiornis*, *Sulcavis* and *Zhouornis* in some major anatomical features, but detailed comparison indicates they represent two new species. We provide morphological and phylogenetic support for a new family, Bohaiornithidae that includes the new species alongside *Bohaiornis*, *Shenqiornis*, *Sulcavis* and *Zhouornis*.

**Institutional abbreviations** BMNH, Beijing Museum of Natural History, Beijing, China; CAGS-IG, Chinese Academy of Geological Sciences, Institute of Geology, Beijing, China; CNU, Capital Normal University, Beijing, China; DNHM, Dalian Natural History Museum, Dalian, Liaoning, China; FRDC, Fossil Research and Development Center, Third Geology and Mineral Resource Exploration Academy, Gansu Provincial Bureau of Geology and Mineral Development, Lanzhou, China; GMV, National Geological Museum of China, Beijing, China; IVPP, Institute of Vertebrate Paleontology and Paleoanthropology,

Chinese Academy of Sciences, Beijing, China; **LP**, Institut d'Estudis Ilerdencs, Lleida, Spain; **LPM**, Liaoning Paleontology Museum, Shenyang, Liaoning, China.

## 2 Materials and methods

Anatomical terminology primarily follows Baumel and Witmer (1993), using English equivalents for the Latin terms. Terminology for structures not named therein follows Howard (1929). Measurements for long bone were taken along the longitudinal axis of the bone in question; for unguis lengths, the measurement represent the linear distance between the tip of the horny sheath (the impression of the sheath was used, when necessary) and ventralmost point of the flexor process or proximal face when the process is poorly developed. The claw curvature of pedal digit III is measured applying the methods of Feduccia (1993). A complete list of measurement is given in Table 1.

**Table 1** Measurements of the holotype and referred specimen of *Parabohaiornis martini* gen. et sp. nov. (IVPP V 18691, V 18690), *Longusunguis kurochkini* gen. et sp. nov. holotype (IVPP V 17964), and *Bohaiornis*

Taxon	referred specimen (IVPPV 17963)							
	V 18691	V 18690	V 17964	V 17963	<i>Bohaiornis</i>	<i>Sulcavis</i>	<i>Zhouornis</i>	<i>Shenqiornis</i>
Skull length	42.5		33.9*	45.3	38.5	42.8		
Coracoid length	21.9	25.6	24.2	25.9	23	24.8	28.4	26.3
Coracoid distal width	12.3	12.9*	12.2	13.1	12.8	12.1		10.7
Scapula length	33.3		34.7	33.9*	36*	34.9	40.7	
Furcula length	26.1		26.3	13.2	24.0	27.5		28.4
Hypocleidium length	7.9		7.3	6.7		8.3		9.0
Sternum length			31.1	36.2	36.4			28.9
Humerus length	43.4	46.7	40.3	50.3	47*	46.5	50.6	46.0
Ulna length	43.8		43.6	53.0	48	51.1	54.0	46.4
Radius length	40.3		40.5	48.8	45.4	47.7	51.4	45.5
Alular metacarpal	3.9		3.6	4.0	4.0	4.5	4.1	4.9
Major metacarpal	16.5		16.8	22.8	21.3	20.8*		20.0
Minor metacarpal	17.6		18.0		22.7	22.2*		20.3
Alular digit 1 length	8.1		7.1	9.3	9.5	9.5	9.1	9.1
Alular digit 2 length	3.5		4.5	5.1	4.5	4.1	4.7	3.4
Major digit 1 length	10.2		10.5	11.1	10.8	11.3	10.8	10.9
Major digit 2 length	7.4		6.9	7.0	7.5	8.0	8.1	7.5

Continued

Taxon	V 18691	V 18690	V 17964	V 17963	<i>Bohaiornis</i>	<i>Sulcavis</i>	<i>Zhouornis</i>	<i>Shenqiornis</i>
Major digit 3 length	3.2		3.4*	3.4	3.6	3.4	3.2	3.4
Minor digit 1 length	5.5		5.2	6.7	5.5	6.1	5.6	5.2
Pygostyle length	18.0	21.8	22.8		18.5*	19.3	17.3	
Ilium length	23.7	24.4		24.2	25.6	26.5		
Pubis length	31.0	32.0	29.1		33.0			32.8
Ischium length	20.3	20.8	17.0		21.0			16.6
Femur length	36.0	37.5	35.8	42.6	39.0	41.3	44.5	
Tibiotarsus length	40.0	45.0	41.8	49.4	46.0	47.3	52.1	
Metatarsal II length	17.1	20.4	19.6		20.8	21.6	24.6	20.7
Metatarsal III length	19.5	22.0	21.4		22.5	24.3	26.1	23.4
Metatarsal IV length	18.1	20.6	20.2		21.8	22.6	24.7	21.3
Digit I-1 length	5.4	6.1	5.4		6.0	7.0	6.3	6.6
Digit I-2 length	6.0	6.3*			7.6	7.2	7.8	
Digit II-1 length	4.5	5.8	5.4	6.1	5.6	8.4	6.3	6.2
Digit II-2 length	6.8	7.6	7.2	8.1	7.1	6.3	8.3	7.3
Digit II-3 length	8.7	10.0		10.2	11.0	9.0	9.9	
Digit III-1 length	6.4	7.8	7.0		7.6	8.2	7.7	8.1
Digit III-2 length	5.4	6.5	6.4	6.5	6.6	7.2	7.1	
Digit III-3 length	5.3	6.6	6.7	6.6	6.5	7.7	7.1	
Digit III-4 length	8.8	11.5	12.0	10.5	11.0		11.1	
Digit IV-1 length	2.9	2.9	3.7	3.8	3.6	4.5	4.2	
Digit IV-2 length	2.6	2.6	2.9	3.5	3.3	3.1	4.0	
Digit IV-3 length	2.9	2.9	3.4	3.2	3.5	3.3	3.3	
Digit IV-4 length	4.1	4.4	4.6	4.4	4.2	4.9	4.3	
Digit IV-5 length	4.7*	7.0		8.7	6.5	7.8	7.3	

Note: *Bohaiornis* holotype (LPM B00167) was measured from the illustration in Hu et al., 2011; measurements for the holotypes of *Sulcavis*, *Shenqiornis* and *Zhouornis* were taken directly from the literature or, where necessary, from illustrations (Wang et al., 2010; O'Connor et al., 2013; Zhang et al., 2013); \* estimated value.

### 3 Systematic paleontology

#### **Aves Linnaeus, 1758**

#### **Ornithothoraces Chiappe, 1996**

#### **Enantiornithes Walker, 1981**

#### **Bohaiornithidae fam. nov.**

**Type genus** *Bohaiornis* Hu et al., 2011.

**Type species** *Bohaiornis guoi* Hu et al., 2011.

**Referred specimens** IVPP V 17963 (Li et al., in press).

**Included genera** *Shenqiornis* Wang et al., 2010; *Bohaiornis* Hu et al., 2011; *Sulcavis* O'Connor et al., 2013; *Zhouornis* Zhang et al., 2013; *Parabohaiornis* gen. nov., and *Longusunguis* gen. nov.

**Diagnosis** Medium size enantiornithines with the following unique combination of features: robust rostrum; large, robust, subconical teeth with sharply tapered and slightly caudally recurved tips; sternum with lateral trabecula strongly projecting caudolaterally; omal tips of furcula with blunt expansions visible in ventrolateral view; scapular blade with convex dorsal margin and straight to weakly concave ventral margin; pygostyle tapered, without abrupt distal constriction; pedal digit II more robust than other digits; pedal unguis extremely elongated with digit III unguis measuring more than 40% length of tarsometatarsus.

**Phylogenetic definition** The most recent common ancestor of *Shenqiornis mengi* and *Bohaiornis guoi*, and all its descendants.

**Locality and horizon** Fengning County, Hebei Province, China, Qiaotou Formation (corresponding to Dawangzhangzi bed of Yixian Formation, Jin et al., 2008); Lamadong Town, Jianchang County and Chaoyang County, Liaoning Province, China. The Lower Cretaceous outcrops near Lamadong Town represent the Jiufotang Formation, with the Yixian Formation largely unexposed in this area (He et al., 2004; Wang X L personal communication). We consider all bohaiornithids to be Early Cretaceous (Aptian) in age (125–120 Ma, He et al., 2004). *Shenqiornis* was from the Qiaotou Formation, equivalent to the Yixian Formation according to Jin et al. (2008); *Sulcavis*, *Bohaiornis*, *Parabohaiornis* and *Longusunguis* were all from the Jiufotang Formation (*contra* Hu et al., 2011 and O'Connor et al., 2013); Zhang et al. (2013) stated that *Zhouornis* was also possibly from the Jiufotang Formation but the provenance needed to be confirmed.

#### ***Parabohaiornis martini* gen. et sp. nov.**

(Figs. 1–6)

**Holotype** IVPP V 18691, a nearly complete and partially articulated skeleton, preserved in a single slab (Fig. 1), which most likely represents a subadult individual based on the absence of fusion in some compound bones (e.g., carpometacarpus, tibiotarsus and tarsometatarsus).



**Referred specimen** IVPP V 18690, an articulated partial skeleton (missing the skull, ulna, radius and hands), preserved in a single slab (Fig. 2). The degree of fusion in compound bones (e.g. carpometacarpus and tarsometatarsus) indicates subadult status, although this specimen appears to be more mature than the holotype.

**Etymology** The generic name is derived from the Latin prefix ‘*para*’ to indicate similar morphology with bohaiornithids. The specific name is in honor of the late Prof. Larry D. Martin, a paleontologist who made great contributions to the study of the evolution of birds during the course of his life.

**Locality and horizon** Lamadong Town, Jianchang County, Liaoning Province, northeastern China; Lower Cretaceous, Jiufotang Formation (He et al., 2004).

**Differential diagnosis** *Parabohaiornis martini* is a bohaiornithid enantiornithine that differs from other bohaiornithids in possessing the following combination of features: three and four teeth on premaxilla and maxilla respectively; nasal without maxillary process (process present in *Longusunguis*, *Zhouornis* and *Sulcavis*); intercondylar incisure absent on tibiotarsus (present in *Sulcavis* and *Bohaiornis*); acromion process parallel to scapular shaft (distinctly deflected dorsally in *Longusunguis* and *Sulcavis*); length ratio of pygostyle to metatarsal III of 0.92–0.99 (*Longusunguis* = 1.06; *Sulcavis* = 0.79; *Zhouornis* = 0.66; estimated to be 0.82 in *Bohaiornis*); and proximal phalanx much shorter than penultimate phalanx in digit IV (less than 70% of length of penultimate phalanx; more than 80% in other bohaiornithids).

**Remarks** V 18690 is identical to the *Parabohaiornis martini* holotype in morphology, visibly preserving all post-cranial features that distinguish this genus from other bohaiornithids, e.g., straight acromion process and tibiotarsus lacking intercondylar incisure.

#### 4 Description

The following description is based on the holotype, except where particular information is stated to be from the referred specimen.

**Skull** The skull is exposed in left lateral view (Fig. 3). Only the left premaxilla is visible, and the right nasal obscures the frontal (nasal) processes so it cannot be determined to what degree the premaxillae are fused. The frontal process of the premaxilla fails to reach the frontal as in *Bohaiornis*, *Longusunguis* and *Sulcavis* (unassessable in *Zhouornis* and *Shenqiornis*). However, the frontal process extends beyond the midpoint of the antorbital fenestra as in *Longusunguis* and *Bohaiornis* (Figs. 3 and 8), making the process longer than in *Zhouornis* and some other enantiornithines, e.g., *Pengornis* and *Eoenantiornis* (Zhou et al., 2005, 2008; O’Connor and Chiappe, 2011; Zhang et al., 2013). The frontal process of *Shenqiornis* appears to be shorter than in other bohaiornithids (Wang et al., 2010), but poor preservation makes this difference equivocal. As in other bohaiornithids, the rostrum is robust. The frontal process defines an approximately 26° angle with the maxillary process, in contrast with the pointed and delicate form seen in many other enantiornithines, e.g., *Rapaxavis*,

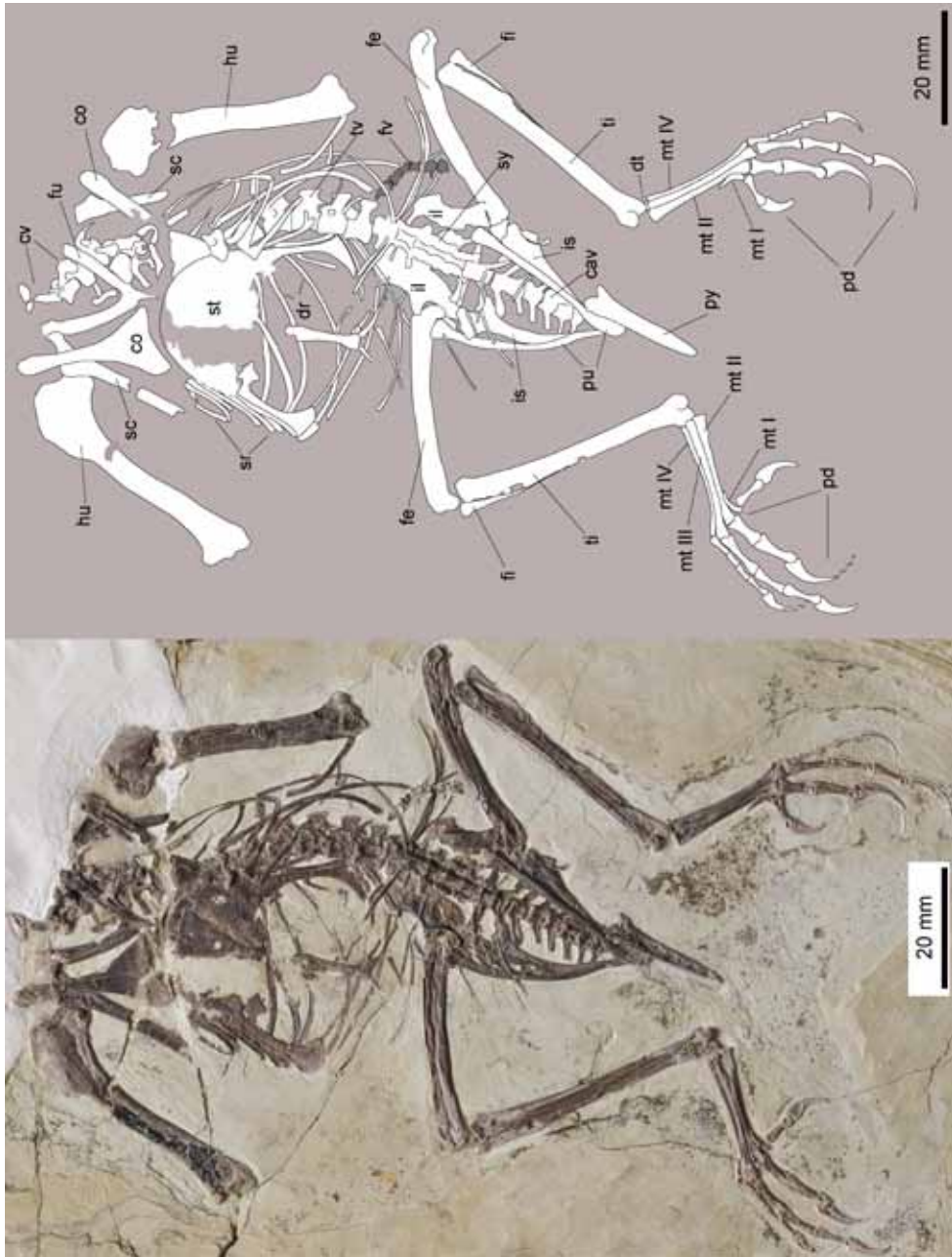


Fig. 2 Photograph and line drawing of *Parabotiatormis martini* gen. et sp. nov. referred specimen (IVPP V 18690)

Abbreviation: fv. vertebrae of fish 鱼的椎体; other abbreviations follow Fig. 1



*Longipteryx*, *Cathayornis* and *Protopteryx*. The maxillary process of the premaxilla is fully exposed laterally and overlies the rostral end of the premaxillary ramus of the maxilla, as in a referred specimen of *Bohaiornis* IVPP V 17963 (Li et al., in press). The premaxillary corpus and maxillary process are short and the facial exposure of the premaxilla is limited, as in most other enantiornithines. Unlike the simple, caudally tapered maxillary process in other enantiornithines, e.g., *Eoenantiornis*, *Longipteryx*, *Rapaxavis* and *Cathayornis*, the maxillary process of *Parabohaiornis* has a complex caudal end: the dorsal margin is longer than the ventral margin, and the ventral margin is interrupted by a notch that slants caudoventrally. The same configuration is visible in a referred specimen of *Bohaiornis* V 17963 and the holotype of *Longusunguis*. In *Zhouornis* the caudal end of the maxillary process is forked, with a short branch present ventral to the long dorsal branch (Zhang et al., 2013); the caudal end of the premaxillary process is poorly preserved and thus prevents comparison with *Shenqiornis* and *Sulcavis*. There are three premaxillary teeth, rather than the four typical in other enantiornithines including *Bohaiornis* (verified from the *Bohaiornis* referred specimen V 17963, Fig. 3; Hu et al., 2011; O'Connor and Chiappe, 2011); three premaxillary teeth are present *in situ* in *Sulcavis*, *Shenqiornis* and *Zhouornis*, although an additional tooth was probably present in each of these taxa, based on either a visible alveolus or gap in the tooth row (Wang et al., 2010; O'Connor et al., 2013; Zhang et al., 2013). However, the exact premaxillary tooth count still remains equivocal in these taxa, and it is possible that Bohaiornithidae is characterized by a reduced premaxillary dentition. The first tooth is reduced in size relative to the caudal two, as in other bohaiornithids (Wang et al., 2010; fig. 2 in Hu et al., 2011; O'Connor et al., 2013; Zhang et al., 2013; fig. 3 in Li et al., in press).

The dorsal process of the maxilla extends caudally to the level of the lacrimal, and forms the entire rostral and rostradorsal margins of the antorbital fenestra; this condition is shared by many enantiornithines, including *Bohaiornis*, *Longusunguis*, *Shenqiornis* and *Zhouornis* (poorly preserved in *Sulcavis*). No maxillary fenestrae are present on the dorsal process. Four maxillary teeth are present, all situated in the rostral half of the maxilla with the caudalmost tooth level with the rostral portion of the antorbital fenestra. Three maxillary teeth have been reported in the poorly preserved maxilla of the *Bohaiornis* holotype (fig. 2 in Hu et al., 2011) while two teeth are preserved in the complete maxilla of a referred specimen of *Bohaiornis* (Li et al., in press); although obscured by poorly preserved maxilla, four teeth are considered to be present in *Sulcavis*, *Shenqiornis* and *Zhouornis* (Wang et al., 2010; O'Connor et al., 2013; Zhang et al., 2013). The right and left nasals are exposed in their medial and lateral views, respectively. The premaxillary process of the nasal tapers rostrally and extends to the rostral border of the naris, as in *Bohaiornis* (Li et al., in press). The same condition appears to be present in *Zhouornis*, but the fact that the caudal part of the skull is crushed against dorsally and rostrally makes this interpretation equivocal. The premaxillary process is relatively shorter in *Longusunguis* (Fig. 8). As in *Shenqiornis* and *Bohaiornis* (verified from *Bohaiornis* referred specimen V 17963, Fig. 3), the nasal lacks a maxillary process, although this feature is present

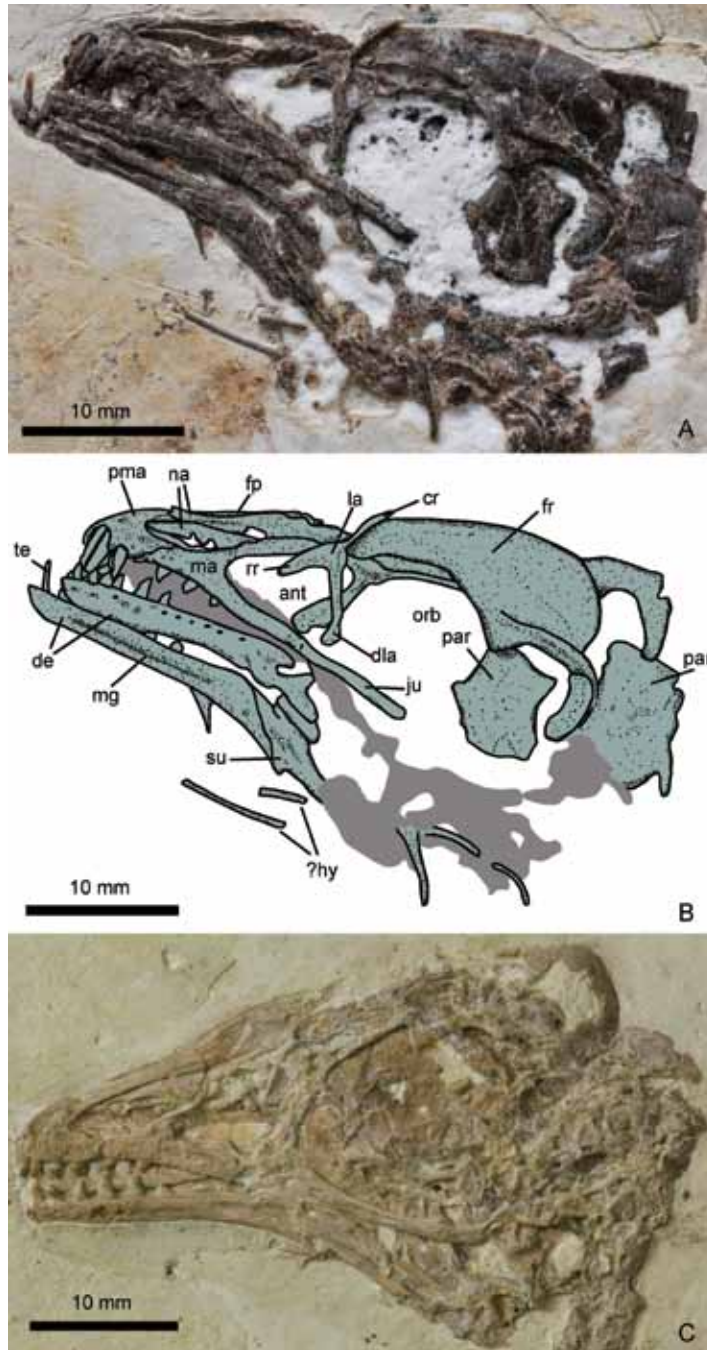


Fig. 3 Photograph (A), line drawing (B) of the skull of *Parabohaiornis martini* gen. et sp. nov. holotype (IVPP V 18691), and the skull of a referred specimen of *Bohaiornis* IVPP V 17963 (C)

Abbreviations: ant. antorbital fenestra 眶前孔; cr. caudal ramus of lacrimal 泪骨后支; de. dentary 齿骨; dla. descending ramus of lacrimal 泪骨下降支; fp. frontal process of premaxilla 前颌骨额突; fr. frontal 额骨; hy. hyoid 舌骨; ju. jugal 颧骨; la. lacrimal 泪骨; ma. maxilla 上颌骨; mg. Meckel's groove 麦氏凹槽; na. nasal 鼻骨; orb. orbit 眼眶; par. parietal 顶骨; pma. premaxilla 前颌骨; rr. rostral ramus of lacrimal 泪骨前支; su. surangular 上隅骨; te. teeth 牙齿

in *Longusunguis*, *Zhouornis* and *Sulcavis*. The maxilla-nasal contact is unclear.

Both the lacrimals are well preserved, the left in lateral view and the right in medial view. The bone is 'T' shaped with the descending ramus longer than either of the dorsal rami, as in other known enantiornithines as well as a subsets of non-avian theropods (e.g., *Velociraptor*, *Tsaagan* and *Sinornithosaurus*; Barsbold and Osmólska, 1999; Xu and Wu, 2001; Norell et al., 2006). The rostral ramus is rostroventrally oriented while the caudal ramus is dorsocaudally oriented. Additionally, the caudal ramus is more steeply inclined than the rostral one. The dorsal margin is strongly concave between the rostral and caudal rami, as in *Pengornis* (O'Connor and Chiappe, 2011). In lateral view, the rostral and caudal rami differ in configuration: the rostral ramus is mediolaterally compressed, with a convex dorsal margin and a tapered rostral end; whereas, the caudal ramus is straight and dorsoventrally compressed. In *Zhouornis* and the referred specimen of *Bohaiornis* V 17963, the lacrimal shows an identical condition (Zhang et al., 2013; Li et al., in press), but this element is not preserved in *Sulcavis* and *Shenqiornis*. A similar lacrimal morphology is also present in a subsets of non-avian theropods (e.g., *Velociraptor*, *Tsaagan* and *Sinornithosaurus*; Barsbold and Osmólska, 1999; Xu and Wu, 2001; Norell et al., 2006). In the enantiornithine LP 4450, by contrast, the rostral and caudal rami both appear to be mediolaterally compressed (O'Connor and Chiappe, 2011). The caudal ramus articulates with the ventral aspect of the frontal. The lateral margin of the frontal, dorsal to the caudal ramus of the lacrimal, forms a distinct rim that projects laterally as in *Pengornis* (O'Connor and Chiappe, 2011), and covers the caudal ramus of the lacrimal in dorsal view. The caudal ramus is mediolaterally wider than the rostral ramus. The lateral margin of the caudal ramus is continuous with the caudolateral margin of the descending ramus. Therefore, the medial margin of the descending ramus is wider than its lateral margin, giving the element an 'L' shaped cross section. Although the caudal ramus is covered by the nasal in the holotype of *Pengornis*, the descending ramus shows the same 'L' shaped cross section as in *Parabohaiornis*, suggesting the caudal ramus was also ventrodorsally compressed. The articulation between the maxilla and jugal is obscured by compression, and due to slight disarticulation it cannot be determined which bone the descending process contacts ventrally (although as preserved it articulates with the jugal).

The frontal is pentagon shaped, elongated rostrocaudally and the caudal end is expanded as in other Mesozoic birds. The caudolateral margin bears a rounded and vaulted process, similar to *Pengornis*. This process is continuous with a ridge, medially delimited by a groove. Although not well preserved, the vaulted process and groove are discernible in the referred specimen of *Bohaiornis* V 17963 (fig.3 in Li et al., in press). The parietals are not fused with the frontals, and a fragment of the right parietal is disarticulated and displaced into the orbit. The right parietal is quadrangular; the medial margin is longer than the lateral margin. The occipital region is poorly preserved.

The two dentaries are not fused with each other and no predentary bone is present, as in other enantiornithines. The left dentary is exposed in lateral view, and the right in medial view.

Meckel's groove is visible on the right dentary. As in *Bohaiornis* and *Longusunguis*, the groove is centrally located, failing to reach either the rostral or caudal end (fig. 3 in Hu et al., 2011; fig. 3 in Li et al., in press); whereas it is more caudally restricted in *Sulcavis* (O'Connor et al., 2013). As in other enantiornithines, the dentary is unforked forming a caudal sloping facet for articulation with the angular and surangular (O'Connor and Chiappe, 2011). The dorsal margin of the dentary is straight, and the ventral margin gently curves ventrally as it extends caudally, as in other bohaiornithids. Five dentary teeth are present in situ, restricted to the rostral half of the left dentary. The caudalmost tooth on the right dentary is more caudally positioned than the fifth tooth on the left dentary (which is followed by an empty alveolus) and is not followed by any visible alveoli, thus we consider six teeth were present in each dentary during life as in *Bohaiornis*, *Longusunguis* and *Zhouornis* (Li et al., in press; contra to Hu et al., 2011; Zhang et al., 2013). In contrast, at least seven dentary teeth are estimated to have been present in *Shenqiornis*, and eight to ten in *Sulcavis* (Wang et al., 2010; O'Connor et al., 2013). The dentary teeth are morphologically similar to those of the upper jaw as in other bohaiornithids. The teeth have long roots, are slightly constricted at the bases of their fat, subconical crowns, and have tapered tips that are slightly caudally recurved. The postdentary bones are poorly preserved. The angular is preserved in articulation with the ventral edge of the surangular. The surangular is more than twice the dorsoventral width of the angular, recalling the condition in *Bohaiornis* (Li et al., in press).

**Axial skeleton** Eight cervicals are preserved in articulation; due to poor preservation of the cranialmost cervicals, the total number of cervicals is unclear (Fig. 1). Nine to eleven cervicals were reported in other enantiornithines with completely preserved neck, e.g., *Sinornis*, *Longipteryx*, *Eoenantiornis* and *Pengornis* (Chiappe and Walker, 2002; Zhou et al., 2005, 2008). We estimate that there are eleven thoracic vertebrae, based on the preserved number of thoracic ribs. The first thoracic vertebrae bears a ventral process, as in basal ornithuromorphs (e.g. *Schizooura*) and living birds, for attachment of the caudal part of m. longus colli ventralis (Bellairs and Jenkin, 1960). Poor preservation and lack of exposure make the presence of the ventral process uncertain in other bohaiornithids. Groove-like lateral excavations on the centra are visible, as in other enantiornithines (Chiappe and Walker, 2002; Wang et al., 2010; Hu et al., 2011; O'Connor et al., 2013; Zhang et al., 2013; Li et al., in press). On the fourth thoracic the right parapophysis is visible, and is centrally located in the craniocaudal dimension, as in other enantiornithines including other bohaiornithids (Chiappe and Walker, 2002).

The synsacrum is well preserved in the referred specimen V 18690; it is composed of seven vertebrae as in *Protopteryx*, whereas most enantiornithines have eight sacral vertebrae (Chiappe and Walker, 2002; Chiappe et al., 2007a). The number of sacral vertebrae is comparable in other bohaiornithids: six or seven have been reported in the *Bohaiornis* holotype (Hu et al., 2011), and seven or eight in *Bohaiornis* referred specimen V 17963, *Longusunguis* and *Sulcavis* (O'Connor et al., 2013; Li et al., in press). The sacral count is unknown in

*Shenqiornis* and *Zhouornis*. The synsacrum is preserved in ventral view; the transverse processes are laterally directed except in the caudalmost sacral vertebra, in which they are caudolaterally directed as in the caudalmost pairs in *Bohaiornis*, *Longusunguis* and *Sulcavis*. The transverse processes of the sixth sacral are the longest and most robust. A slight groove runs along the ventral surface of the synsacrum, but it is unclear if this is a diagenetic artifact. A transverse lamina is present between the transverse processes although it is poorly developed between the cranialmost two sacra.

There are at least five free caudal vertebrae. The transverse processes of these vertebrae are laterocaudally directed, and exceed the width of the corresponding centra. Moving distally along the tail, the caudals decrease in size and the transverse processes become less caudally directed. The processes are laterally directed in the last free caudal, as in *Longusunguis*. The pygostyle is well preserved in ventral view in the referred specimen V 18690 (Fig. 2). Proximally, the proximoventral processes project farther cranially than the articular facet, as is typical in enantiornithines (Chiappe et al., 2002). Because the ventrolateral process is not continuous caudally with the pygostyle shaft, the ventral surface of the pygostyle is not deeply concave as in *Rapaxavis* and other taxa with well developed ventrolateral processes. The pygostyle of *Parabohaiornis*, like those of other bohaiornithids, is tapered gently distally (Wang et al., 2010; Hu et al., 2011; O'Connor et al., 2013; Zhang et al., 2013; Li et al., in press), without the conspicuous constriction seen in most enantiornithines, including *Rapaxavis*, *Shanweinia*, *Boluochia* and *Halimornis*.

Eleven thoracic ribs and seven sternal ribs are preserved. Uncinate processes are clearly preserved in articulation, though not in a state of fusion with the thoracic ribs. They extend dorsally, defining an acute angle of 40° with the corresponding thoracic rib shafts (Fig. 1). The processes are short, not reaching the next rib, whereas in non-avian dinosaurs and ornithuromorphs the uncinate processes are long enough to cross at least one adjacent rib (Codd et al., 2008; Codd, 2010). They are unexpanded or weakly expanded at the base. Uncinate processes are rarely preserved in enantiornithines, and have been previously reported only in *Longipteryx* and STM 29-8 (Zhang et al., 2001; Zheng et al., 2013a). In both cases the uncinate processes are morphologically similar to those of *Parabohaiornis* (Zhang et al., 2001; Zheng et al., 2013a). Several short and slender elements preserved adjacent to the pubis are interpreted as gastralia. Based on the referred specimen, an estimated four to five pairs of gastralia were present (Fig. 2).

**Thoracic girdle** Only the right side of the thoracic girdle is preserved in the holotype. The strut-like coracoid is exposed in ventral view (Figs. 1 and 2). The supracoracoidal nerve foramen perforates the neck of the coracoid, and opens into a longitudinal groove, which is on the medial surface of the neck of the coracoid, as in such enantiornithines as *Zhouornis*, *Eoalulavis*, *Neuquenornis* and *Enantiornis* (Chiappe and Calvo, 1994; Sanz et al., 1996; Chiappe and Walker, 2002; Zhang et al., 2013). *Parabohaiornis* resembles other enantiornithines in lacking a procoracoid process (Chiappe and Walker, 2002). The lateral

margin is concave for most of its length, but the distal one-sixth of the margin flares outward to form a blunt, convex lateral angle as in other bohaiornithids (Wang et al., 2010; O'Connor et al., 2013; Zhang et al., 2013). This configuration contrasts with the derived condition seen in some enantiornithines, in which the entire lateral margin is convex (Chiappe and Calvo, 1994; Chiappe and Walker, 2002). As in other enantiornithines, a distinct lateral process is absent. The medial margin of the coracoid is entirely concave and forms a blunt medial angle that is more acute than the lateral angle as in other bohaiornithids. As in all bohaiornithids, the sternal margin is weakly concave. As in *Bohaiornis* and *Longusunguis*, the length of the sternal margin is slightly greater than half that of the coracoid, larger percentage than in *Sulcavis* and *Shenqiornis* (Fig. 4; Table 1).

The scapula is shorter than the humerus, and has a weakly tapered distal end. As in *Longusunguis*, and most likely *Shenqiornis*, the straight scapular shaft has a convex dorsal margin and a straight ventral margin; in contrast, the scapula is slightly curved ventrally in a parasagittal plane in *Zhouornis* and IVPP V 18631, as in some basal ornithuromorphs and neornithines (Zhang et al., 2013; Wang et al., in press b). The acromion is elongate, exceeding the length of the humeral articular facet of the scapula. As in some enantiornithines, e.g., *Protopteryx*, *Longipteryx*, *Longirostravis*, *Concornis* and *Eocathayornis*, the acromion is blunt,

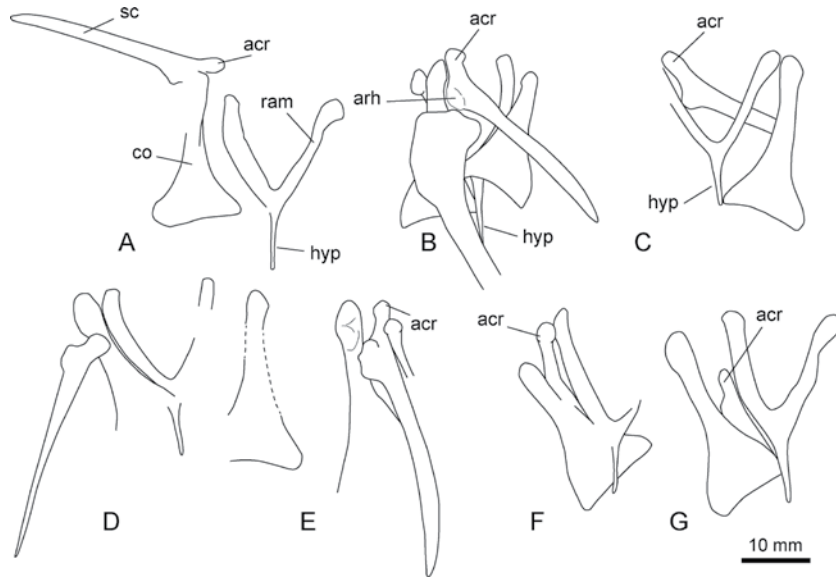


Fig. 4 Bohaiornithid pectoral girdle

A. *Parabohaiornis martini* gen. et sp. nov. holotype (IVPP V 18691); B. *Longusunguis kurochkini* gen. et sp. nov. holotype (IVPP V 17964); C. *Bohaiornis* holotype (LPM B00167); D. a referred specimen of *Bohaiornis* (IVPP V 17963); E. *Zhouornis* holotype (CNUVB 0903); F. *Sulcavis* holotype (BMNH ph-000805); G. *Shenqiornis* holotype (DNHM D2950). Note that the scapula of the referred specimen of *Bohaiornis* is exposed in laterodorsal view and the acromion process is compressed laterally, which causes the acromion process to appear to form a large angle with the shaft

Abbreviations: acr. acromion process 肩峰突; arh. coracoidal articular humeral facet 鸟喙骨上的肱骨关节面; ram. ramus of furcula 叉骨支; hyp. hypocleidium 叉骨突; other abbreviations follow Fig. 1

rather than tapered cranially. In costolateral view, the acromion projects cranially, maintaining an orientation nearly parallel to that of the scapular shaft. This condition is present only in a few enantiornithines, including *Bohaiornis*, *Shenqiornis*, *Zhouornis* and *Concornis* (Fig. 4; Sanz et al., 2002; Wang et al., 2010; fig. 4 in Hu et al., 2011; Zhang et al., 2013). More commonly, the acromion strongly projects craniodorsally, defining a large angle with the shaft, as in, for example, *Longusunguis* and *Sulcavis* (Chiappe and Walker, 2002; Chiappe et al., 2002; Morschhauser et al., 2009; Walker and Dyke, 2009). As can be seen in the right scapula of the referred specimen V 18690, the cranial end of the acromion appears to be mediolaterally expanded as in *Bohaiornis*, *Zhouornis*, *Sulcavis* and some Late Cretaceous enantiornithines (Chiappe et al., 2002; Walker and Dyke, 2009). This feature is difficult to verify in *Longusunguis* and *Shenqiornis*.

The furcula is 'Y' shaped with an interclavicular angle of  $60^\circ$  as in *Bohaiornis* and *Sulcavis* (Hu et al., 2011; O'Connor et al., 2013), but greater than in *Shenqiornis* and *Zhouornis* ( $50^\circ$  and  $45^\circ$ , respectively; Wang et al., 2010; Zhang et al., 2013). The hypocleidium is more than half the length of the either furcular ramus (less in *Bohaiornis*). The furcula is exposed in ventral view, although the left ramus appears to be slightly crushed and distorted so that it is in ventrolateral view. The ramus is 'L' shaped in cross section, with the ventral margin wider than the dorsal margin, as in other enantiornithines (Chiappe and Walker, 2002). The lateral margins of the rami are convex in ventral view while the medial margins are straight, making the furcula similar in shape to those of *Bohaiornis* (fig. 4 in Li et al., in press), *Shenqiornis*, *Concornis* and *Pengornis*. The omal tip, exposed on the left ramus of the holotype, appears to be bluntly expanded into an articular facet, a feature also present in other bohaiornithids (Fig. 7). The hypocleidium is ventrally keeled, as in *Bohaiornis*, *Shenqiornis* and *Longusunguis* (Wang et al., 2010; fig. 4 in Hu et al., 2011). The hypocleidium is not exposed in the holotype and only known specimen of *Zhouornis*.

The sternum is not completely preserved in either the holotype or the referred specimen V 18690 (Fig. 5). The following description is based on a combined reconstruction incorporating information from both specimens. The rostral margin is rounded and parabolic, similar to its counterpart in *Bohaiornis*, *Longusunguis* and *Longipteryx*, and the sternum lacks the angular cranio-lateral margins reported in *Zhouornis* and *Shanweinia* (O'Connor et al., 2009; Zhang et al., 2013). Six sternal ribs remain in articulation with the left side of the sternum in the referred specimen V 18690. In the holotype, there are six thoracic ribs preserved in articulation with the corresponding sternal ribs. Cranio-lateral and lateral processes are absent. Caudally, there are two pairs of trabeculae. As in *Bohaiornis* and *Shenqiornis*, the lateral trabecula is strongly caudolaterally directed, defining a large angle with the longitudinal axis of the sternum (*Parabohaiornis* holotype:  $21^\circ$ , referred specimen V 18690:  $22^\circ$ ; *Bohaiornis* holotype:  $20^\circ$ , referred specimen IVPP V 17964:  $23^\circ$ ; *Shenqiornis*: estimated  $16^\circ$ ); similar condition is evident in *Zhouornis*, *Elsornis*, *Vescornis* and *Longipteryx*, but the lateral trabecula is less laterally directed and forms a smaller angle with the longitudinal axis (*Longipteryx*:

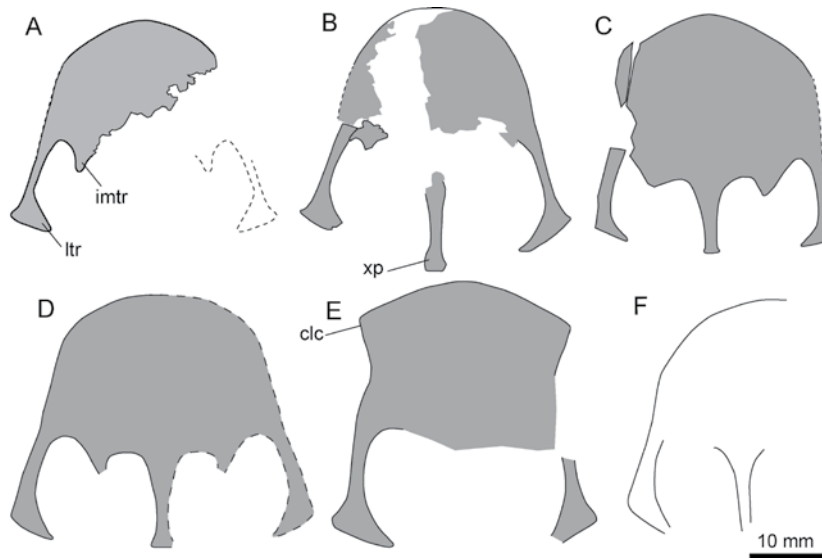


Fig. 5 Bohaiornithid sternum

A. *Parabohaiornis martini* gen. et sp. nov. holotype (IVPP V 18691); B. a referred specimen (IVPP V 18690); C. *Bohaiornis* holotype (LPM B00167); D. a referred specimen (IVPP V 17963); E. *Zhouornis* holotype (CNUVB 0903); F. *Shenqiornis* holotype (DNHM D2950)

Abbreviations: clc. cranio-lateral corner 前外侧角; imtr. intermediate trabecula 中间突; ltr. lateral trabecula 外侧突; xp. xiphoid process 剑状突

11°; *Vescornis*: 9°; *Elsornis*: 8°; *Zhouornis*: 7°). The distal end of the lateral trabecula bears a triangular expansion with an acute medial angle, a feature otherwise only known in *Bohaiornis* and *Zhouornis* among enantiornithines. The impression of the left lateral trabecula in *Shenqiornis* suggests a similar triangular expansion, but the distal expansion is poorly preserved in other bohaiornithids. The intermediate trabecula is small, short, and triangular, as in most other enantiornithines. The xiphoid process projects farther caudally than the lateral trabecula, whereas these two elements are equal in caudal extent in *Bohaiornis* (Hu et al., 2011; Li et al., in press; unclear in other bohaiornithids). The xiphoid process flares slightly mediolaterally at the distal end, as in *Bohaiornis*, *Longirostravis* and IVPP V 18631 (Li et al., in press; Wang et al., in press b). In *Eoalulavis* and *Liaoningornis*, the distal end of the xiphoid process is strongly mediolaterally expanded (Sanz et al., 1996; Zhou and Hou, 2002; O'Connor, 2012), giving the process an inverted 'T' shape.

**Thoracic limbs** The forelimbs are fully articulated (Fig. 1). The humerus is slightly shorter than the ulna and twisted so that the proximal and distal ends are in different planes, as in other bohaiornithids and many other enantiornithes. The proximal margin displays the typical enantiornithine condition: the central part of the head is concave and bounded by elevated dorsal and ventral regions (Chiappe and Walker, 2002). This topology is shared by other bohaiornithids except *Zhouornis*, in which the proximal margin is reported to be flat (Zhang et al., 2013). The deltopectoral crest projects dorsally and is dorsoventrally narrower



than the humeral shaft. As in *Bohaiornis* and *Zhouornis*, the deltopectoral crest extends along the proximal third of the humerus before receding gently into the shaft (Figs. 1 and 2; fig. 1 in Hu et al., 2011; fig. 4 in Li et al., in press). The crest ends more abruptly in *Sulcavis*, *Shenqiornis* and *Longusunguis*. The distal surface of the humerus is angled ventrally and forms a small flexor process, as in other bohaiornithids and some other enantiornithines, including *Vescornis*, *Longipteryx* and IVPP V 18586 (Zhang et al., 2001, 2004; Wang et al., in press a; fig. 1 in Li et al., in press). The condyles are oval, with their long axes perpendicular to the humeral shaft, and the dorsal condyle is larger than the ventral condyle. In the referred specimen V 18690, a depression visible on the cranial surface of the right humerus may represent the brachialis fossa.

The ulna is bowed proximally and becomes straight distally, creating an interosseous space between the ulna and the radius as in all enantiornithines. The radius is straight and bears an elongate longitudinal groove on the interosseous surface as in *Bohaiornis*, *Longusunguis*, *Zhouornis* and some other enantiornithines (Chiappe and Walker, 2002; Hu et al., 2011; Zhang et al., 2013; Li et al., in press; Fig. 1).

The ulnare is triangular with a shallow metacarpal incisure, and the radiale is quadrangular and appears smaller than the ulnare, consistent with other bohaiornithids (the two carpals are not well preserved in *Shenqiornis*). The semilunate carpal contacts the major metacarpal but is not fused with the latter bone, most likely due to the subadult ontogenetic status of the specimen.

Both hands are preserved in dorsal aspect. The alular metacarpal is small and bears a ginglymoid articular facet for the proximal phalanx. No extensor process is present. As in other bohaiornithids, the proximocranial corner of the alular metacarpal is rounded, rendering the proximal margin substantially narrower than the distal margin. The major and minor metacarpals are unfused proximally, further suggesting subadult status. The proximal margin of the minor metacarpal lies distal to that of the major metacarpal, as in other bohaiornithids (Wang et al., 2010; O'Connor et al., 2013; Zhang et al., 2013). A longitudinal depression is on the dorsal surface of the major metacarpal, a feature that is also discernible in other bohaiornithids; based on the morphology and position of the depression, we interpret it as the sulcus tendineus. The minor metacarpal is dorsoventrally wider than its craniocaudally thick, as in *Bohaiornis*, *Zhouornis*, *Longusunguis* and some other enantiornithines including *Cathayornis* and *Rapaxavis* (O'Connor and Dyke, 2010; O'Connor et al., 2011c). The minor metacarpal is bowed caudally, and the distal end slightly wraps around the distal end of the major metacarpal. As is typical in enantiornithines, the minor metacarpal extends farther distally than the major metacarpal (Chiappe and Walker, 2002). An intermetacarpal space is absent.

The manual phalangeal formula is 2-3-1. The alular digit extends distally to the level of the distal end of the major metacarpal, as in other bohaiornithids, *Eoenantiornis* and V 18631 (Zhou et al., 2005; Hu et al., 2011; Wang et al., in press b). As in other bohaiornithids, the

alular claw is larger than the major claw (Wang et al., 2010; O'Connor et al., 2013; Zhang et al., 2013). The proximal phalanx of the major digit is rectangular, with unexpanded ends, and is the most robust phalanx in the hand. The proximal phalanx develops a beveled caudodistal corner, as in other bohaiornithids (Wang et al., 2010; O'Connor et al., 2013; Zhang et al., 2013; fig. 2 in Li et al., in press). Only one phalanx is preserved in the minor digit, although this may be an artifact of preservation. A very reduced second phalanx, seen in enantiornithine taxa including *Rapaxavis*, *Longipteryx*, *Protopteryx*, *Shenqiornis* and *Zhouornis* (Zhang and Zhou, 2000; Zhang et al., 2001; Morschhauser et al., 2009; Wang et al., 2010; Zhang et al., 2013), may have been present.

**Pelvic girdle** The following description is based on the well preserved pelvis of the referred specimen V 18690. The pelvic girdle is poorly preserved or covered in other reported bohaiornithids, limiting the potential for comparison (Wang et al., 2010; Hu et al., 2011; O'Connor et al., 2013; Zhang et al., 2013; Li et al., in press). The pelvic elements are not fused to each other around the margin of the acetabulum. The ilia are preserved in ventral view and are not fused to the synsacrum. Each ilium has a convex dorsal margin. The preacetabular ala is longer than the postacetabular ala, as in *Bohaiornis* and other enantiornithines (Chiappe and Walker, 2002; Hu et al., 2011; Li et al., in press). The pubic peduncle is hook-like and longer than the ischiadic peduncle; a similar condition is present in some longipterygids (O'Connor et al., 2009). The pubic peduncle is also long and somewhat curved in the Late Cretaceous enantiornithine *Nanantius valifanovi*, a possible junior synonym of *Gobipteryx minuta* (Kurochkin, 1996). The right ischium is well preserved in both the holotype and the referred specimen V 18690. The ischium is approximately two-thirds the length of the pubis, proportionally longer than in *Shenqiornis* (Wang et al., 2010). The pubic peduncle is much larger than the iliac peduncle as in *Shenqiornis*. The ischium resembles *Sinornis* in that the distal half of the bone is dorsomedially deflected (dorsal surface concave), in contrast with the straight and strap-like ischial blade seen in *Shenqiornis* and V 18631 (Sereno et al., 2002; Wang et al., 2010; Wang et al., in press b). The ischial blade tapers caudally. The proximal dorsal process is well developed, distinct and tab-like, as in other enantiornithines and also the basal pygostylian *Sapeornis* (Zhou and Zhang, 2003b). The dorsal process is slightly cranially deflected and defines a concave margin with the iliac pedicel of the ischium. A similar condition is visible in *Bohaiornis* and *Shenqiornis* (fig. 3i in Wang et al., 2010; fig. 3 in Hu et al., 2011). The pubic shaft is rod-like and nearly straight in ventral view, lying parallel to the ilium and ischium. The dorsal margin of the pubis is slightly concave. The distal end expands into a small pubic foot, as in *Shenqiornis*, *Bohaiornis*, *Zhouornis*, *Longusunguis* and some other enantiornithines (absent in *Qiliania*).

**Hindlimbs** The hindlimb elements are preserved in articulation. The femora are exposed in medial and craniomedial views in the holotype V 18691 and the referred specimen V 18690, respectively. The femoral shaft is slightly bowed cranially. As in *Zhouornis*, the fossa for the capital ligament is not developed. Whereas, the fossa is present in some other

enantiornithines, including *Concornis*, *Rapaxavis* and *Shanweinia* (Sanz et al., 2002; O'Connor et al., 2009, 2011c). The medial condyle of the distal end of the femur is exposed in medial view; in profile it has a flat proximal margin.

In the holotype specimen V 18691, the proximal tarsals are fused to each other but not to the distal end of tibia, from which they are separated by a gap (Fig. 6). The proximal tarsals appear partially fused to the tibia in referred specimen V 18690, which is slightly larger than the holotype, suggesting that a true tibiotarsus was present in adults. The fibular crest extends along the proximal third of the tibia. The distal part of the cranial surface of the tibia lacks an extensor sulcus. The medial and lateral condyles are formed by the proximal tarsals, which also form a triangular ascending process. The condyles are large and bulbous, taper medially, and contact each other rather than being separated by an intercondylar incisure. Whereas the intercondylar incisure is present in *Longusunguis*, *Bohaiornis* and *Sulcavis* (Figs. 6 and 7; Hu et al., 2011; O'Connor et al., 2013). The medial condyle is wider than the lateral one, as in *Bohaiornis*, *Longusunguis* and many other primitive birds (Figs. 6 and 7; Chiappe et al., 1999). Well-developed medial epicondyles are preserved in both tibiotarsi of the referred specimen V 18690, and their apices are approximately level with the proximal margin of the medial condyle in proximodistal dimension; in *Bohaiornis*, *Sulcavis* and *Zhouornis*, the corresponding area is flat (unclear in *Longusunguis* and *Shenqiornis*). The fibula narrows distally and

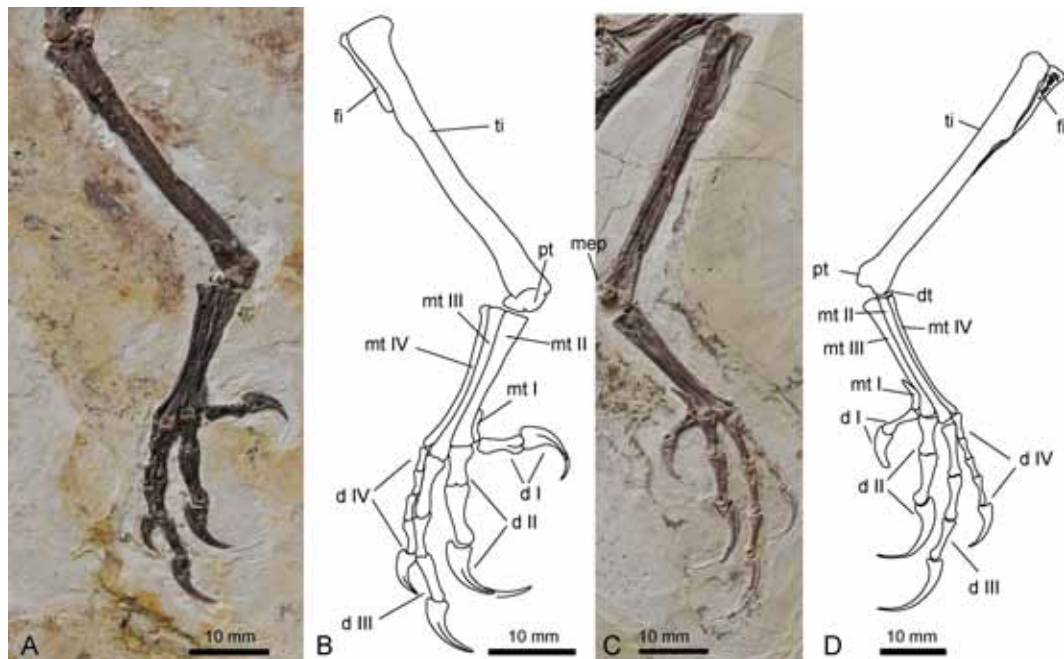


Fig. 6 Photographs and line drawing of the distal parts of the hindlimbs of *Paraboaiornis martini* gen. et sp. nov.

A, B. holotype (IVPP V 18691); C, D. a referred specimen (IVPP V 18690)

Abbreviations: d I-IV. digit I, II, III, IV 第1, 2, 3和4脚趾; mep. medial epicondyle 内上髁; other abbreviations follow Fig. 1

terminates halfway down the tibia as in *Sulcavis*, making the fibula substantially shorter than that of *Pengornis*.

A true tarsometatarsus is absent, in that the distal tarsals are not fused to the metatarsals, and we interpret this condition as a subadult feature (Fig. 6). Poor preservation obscures morphological details of the distal tarsals in the holotype, but a free tarsal is clearly evident in the left foot in both the holotype and the referred specimen V 18690 (Figs. 1 and 6). Free distal tarsals have been definitively reported only in seven Mesozoic avian specimens (Chiappe et al., 2007a; Zhou et al., 2013; Wang et al., in press a), four of which are enantiornithines: the juvenile GMV2158, *Rapaxavis*, *Shenqiornis* and IVPP V 18586 (Chiappe et al., 2007a; Wang et al., 2010; O'Connor et al., 2011c; Wang et al., in press a). In the holotype, a small plate-like tarsal caps metatarsal II. In the referred specimen V 18690, a single proximodistally compressed tarsal completely covers the proximal ends of metatarsals III and IV, without contacting metatarsal II. It appears a second flat tarsal is also fused to the proximal surface of metatarsal II in the referred specimen (Figs. 2 and 6), consistent with the interpretation that this specimen is more mature. Metatarsals II–IV are unfused along their lengths, as is typical in enantiornithines (Chiappe and Walker, 2002). The configuration of the metatarsals is largely similar with other bohaiornithids (Wang et al., 2010; Hu et al., 2011; O'Connor et al., 2013; Zhang et al., 2013; Figs. 6 and 7). Among the metatarsals, metatarsal III is the longest, closely followed by metatarsal IV. Metatarsal II terminates at the proximal margin of the metatarsal III trochlea. The shaft of metatarsal II narrows between the proximal and distal ends, and appears to be transversely narrower than dorsoplantarly deep. Both the proximal end and the trochlea of metatarsal II are wider than those of metatarsal III. As in *Sulcavis* and *Zhouornis*, the trochlea of metatarsal II appears weakly ginglymoid and bears a well developed dorsal trochlear depression; the metatarsal III trochlea is ginglymoid with only a weak dorsal depression. The dorsolateral surface of metatarsal II bears a tubercle for the m. tibialis cranialis, located at approximately one third of the distance from the proximal end (Chiappe, 1996). The tubercle contacts the medial surface of metatarsal III as in *Pengornis* and *Longirostravis* (O'Connor, 2009); the corresponding area is broken in other bohaiornithids. The distal halves of metatarsal II and IV are both curved away from the midline of the foot, as in *Bohaiornis*, *Sulcavis* and *Zhouornis* (Hu et al., 2011; O'Connor et al., 2013; Zhang et al., 2013). This makes the medial and lateral surfaces of the tarsometatarsus slightly concave (Fig. 6), rather than straight as in other enantiornithines, including *Pengornis*, *Concornis*, *Avisaurus* and *Soroavisaurus* (Chiappe, 1993; Sanz et al., 2002; Zhou et al., 2008). Metatarsal IV is the narrowest, an autapomorphy of Enantiornithes (Chiappe and Walker, 2002), and the distal end of this bone is mediolaterally compressed and reduced to a single condyle as in other bohaiornithids and some enantiornithines (not reduced in *Soroavisaurus* and *Avisaurus*). Metatarsal I is short and articulates on the medial surface of metatarsal II as in *Bohaiornis*, *Sulcavis* and *Zhouornis* (fig. 1e in Hu et al., 2011; O'Connor et al., 2013; Zhang et al., 2013). The distal half of metatarsal I is caudomedially deflected and protrudes medially to form an articular surface for the hallux,

giving the metatarsal I ‘P’ shaped morphology in cranial view. The lateral aspect of metatarsal I is visible only in the right foot of the holotype, and is flat rather than concave. No articular fossa for metatarsal I is present on metatarsal II.

The pedal phalangeal formula is 2-3-4-5-x, as in other Mesozoic birds (Fig. 6). The toe proportions and morphology are largely consistent with those of other bohaiornithids, especially in the following respects: digit II is much more robust than the other digits; in digits II and IV, the penultimate phalanx is longer than the proximal phalanges (in *Sulcavis*, the proximal phalanx is longer than the penultimate one in digit II); and the proximal three phalanges of digit IV are subequal in length and are more delicate and shorter than all other non-ungual phalanges in the foot (Table 1). All the phalanges bear deep collateral ligament pits. The feet of *Parabohaiornis*, *Longusunguis*, *Bohaiornis* and *Zhouornis* are distinguished from those of other enantiornithines by the presence of an extremely elongate digit III ungual. This ungual, with its horny sheath, is close to half the length of metatarsal III, proportionally longer than in any other Mesozoic birds (Table 2). One disarticulated ungual measuring

**Table 2 Selected measurements of *Parabohaiornis martini* gen. et sp. nov., *Longusunguis kurochkini* gen. et sp. nov., other bohaiornithids, and other enantiornithines and Jehol birds (mm)**

Taxon	Cv	mt III	Claw	Ratio	Fe(%)	Ti(%)	Tmt(%)	Rtmt
<i>Parabohaiornis</i> V 18691	109°	19.5	8.8	0.45	0.38	0.42	0.20	0.15
<i>Parabohaiornis</i> V 18690	115°	22.0	11.5	0.52	0.36	0.43	0.21	0.14
<i>Longusunguis</i> V 17964	103°	21.4	12.0	0.56	0.36	0.42	0.22	
<i>Bohaiornis</i> LPM B00167	101°	21.4	10.5	0.49	0.37	0.43	0.19	
<i>Shenqiornis</i> DNHM D2950		23.4						0.14*
<i>Sulcavis</i> BMNH ph-000805		24.3			0.37	0.42	0.21	0.13
<i>Zhouornis</i> CNUVB 0903	110°	26.1	11.1	0.43	0.36	0.42	0.22	0.13
<i>Shanweinia</i> DNHM D1878	108°	22.5	8.2	0.36	0.34	0.43	0.23	0.11
<i>Qiliania</i> FRDC-05-CM-006	110°	27.1	8.8	0.32	0.32	0.42	0.26	
<i>Pengornis</i> V 15336	125°	26.8	11.5	0.43	0.38	0.40	0.22	0.18
<i>Sinornis</i> BMNH BPV 538	118°	14.6	4.9	0.34	0.34	0.43	0.23	0.12
<i>Sapeornis</i> DNHM D3078	86°	34.5	9.1	0.26	0.37	0.41	0.22	0.13
<i>Confuciusornis</i> GMV 2130	144°	22.8	6.4	0.28	0.37	0.43	0.20	0.15
<i>Zhongjianornis</i> V 15900	51°	25.3	7.7	0.30	0.33	0.49	0.19	0.17
<i>Schizooura</i> V 16861	56°	35.8	5.5	0.15	0.31	0.43	0.25	0.12
<i>Archaeorhynchus</i> V 17075	20°	20.0	5.1	0.26	0.36	0.42	0.22	0.17

Note: Measurements for *Bohaiornis*, *Shenqiornis*, *Sulcavis*, *Zhouornis*, *Shanweinia*, *Qiliania*, *Sinornis*, *Sapeornis* and *Confuciusornis* were taken from images in the literature (Chiappe et al., 1999; Sereno et al., 2002; O’Conner et al., 2009, 2013; Wang et al., 2010; Ji et al., 2011; Gao et al., 2012; Zhou et al., 2013; Zhang et al., 2013). \* estimated value.

Abbreviations: Cv. curvature of the ungual of pedal digit III; Fe (Ti or Tmt)% = femur (tibiotarsus or tarsometatarsus)/ (femur + tibiotarsus + tarsometatarsus)%; mt III. length of metatarsal III; Ratio = ungual length / mt III; Rtmt = midshaft mediolateral width of tarsometatarsus/tarsometatarsus length.

approximately half the length of metatarsal III is preserved in the holotype of *Shenqiornis*, but it cannot be confirmed that this ungual belongs to the third toe. The third digit ungual is not complete in the holotype of *Sulcavis*, but the preserved part is close in its proportions to those of other bohaiornithids; additionally, the incomplete second ungual is about 36% the length of tarsometatarsus, and all these evidences strongly suggest similar proportions to other bohaiornithids (fig. 7 in O'Connor et al., 2013). The ungual phalanx in each digit, without the horny sheath, is weakly arched compared to those of other Jehol enantiornithines, although still strongly recurved compared to Jehol ornithuromorphs (Table 2). The claws are heterogeneous; the second digit ungual is the most robust, followed by that of the hallux. The ungual of digit IV is smaller than the other unguals as in *Bohaiornis*, *Sulcavis*, *Zhouornis* and *Longusunguis* (fig. 1e in Hu et al., 2011; O'Connor et al., 2013; Zhang et al., 2013), a feature elsewhere only known in *Vescornis*, *Qiliania*, V 18586, and V 18631 among enantiornithines (Zhang et al., 2004; Ji et al., 2011; Wang et al., in press a, b). Longitudinal crests ventral to the neurovascular sulci are present on the unguals, which has been previously reported in other enantiornithines (O'Connor et al., 2009).

**Aves Linnaeus, 1758**

**Ornithothoraces Chiappe, 1996**

**Enantiornithes Walker, 1981**

**Bohaiornithidae fam. nov.**

***Longusunguis kurochkini* gen. et sp. nov.**

(Figs. 7–9)

**Holotype** IVPP V 17964, a complete and articulated skeleton, preserved in a slab (Fig. 7). The absence of fused compound bones, including capometacarpus, tibiotarsus and tarsometatarsus, suggests the specimen is a subadult.

**Etymology** The generic name is derived from the Latin words ‘*longus*’ (long), ‘*unguis*’ (claw), and refers to the distinctly long pedal unguals that characterize this taxon and other bohaiornithids. The specific name is dedicated to the late Prof. Evgeny Kurochkin, an eminent paleornithologist who advanced our understanding about fossil birds.

**Locality and horizon** Lamadong Town, Jianchang County, Liaoning Province, northeastern China; Lower Cretaceous, Jiufotang Formation (He et al., 2004).

**Differential diagnosis** *Longusunguis kurochkini* is a bohaiornithid that can be distinguished from other bohaiornithids by following combination of features: maxilla bearing an accessory fenestra on the jugal process (an accessory fenestra is situated on the dorsal process in *Zhouornis*, and no fenestra is present on the maxilla in other bohaiornithids); descending ramus of the lacrimal bearing elongate excavation on its caudal margin; lateral margin of coracoid more convex than other bohaiornithids; acromion process strongly projecting dorsally; and pygostyle longer than tarsometatarsus.

**Description Skull** The skull is exposed in right lateral view (Fig. 8). The caudoventral

portion of the skull is crushed, preserving no anatomical information, and the caudodorsal portion of the skull (i.e. the brain case) is not preserved. The right premaxilla is preserved in laterodorsal view. The premaxillary corpi appear fused as in some Late Cretaceous enantiornithines (O'Connor and Chiappe, 2011), but the frontal (nasal) processes are unfused although they are tightly articulated medially. The premaxilla and maxilla are preserved in nearly natural articulation. The articular facet for the maxilla recalls the condition in *Parabohaiornis* and *Bohaiornis*: in lateral view, the caudal end of the maxillary process of the premaxilla is 'L' shaped, forming a long dorsal process that overlies the tapered rostral end of the premaxillary process of maxilla. In *Zhouornis* the caudal end of the maxillary process of the premaxilla is forked.

Three premaxillary teeth are preserved, but an additional one could possibly be present given the large gap between the second and third preserved teeth. The rostralmost tooth is smaller than the other teeth, as in other bohaiornithids. The nasals articulate medially but are not fused. The nasal resembles that of *Eoenantiornis* (Zhou et al., 2005) in that the premaxillary and maxillary processes define a broad concave rostral margin, which forms the dorsocaudal margin of the external naris; the equivalent margin is narrower in *Zhouornis* and *Sulcavis* (O'Connor et al., 2013; Zhang et al., 2013). The premaxillary process is slender and longer than the maxillary process. A 'T' shaped element situated dorsal to the nasals is disarticulated and incompletely preserved, rendering identification difficult. We interpret this element as the left lacrimal, preserved in lateral view, based on the following evidence: compared to other enantiornithines, the preserved long ramus is too long to be either the rostral or the caudal ramus of the dorsal ramus, and therefore this long ramus is the descending ramus. The incomplete ramus, which projects ventrally from the descending ramus, is the rostral ramus, because it is mediolaterally compressed, like the rostral ramus in *Parabohaiornis*, *Bohaiornis* and *Zhouornis*. The third and the final ramus is logically the caudal ramus, and the preserved proximal portion is also dorsoventrally compressed as in *Parabohaiornis*, *Bohaiornis* and *Zhouornis*. If this interpretation is correct, then this unique morphology of lacrimal (e.g., caudal and rostral rami compressed in different dimensions) is present in all bohaiornithids (although the lacrimal is not preserved in *Sulcavis* and *Shenqiornis*).

The maxilla forms the majority of the facial margin, as in other bohaiornithids. The dorsal process is caudally inclined to contact the nasal and potentially the lacrimal as in *Parabohaiornis*, *Shenqiornis* and *Bohaiornis*. This process is rostrocaudally compressed and mediolaterally wider than observed in some enantiornithines (e.g. *Rapaxavis*, *Pengornis*), as in *Parabohaiornis*, *Shenqiornis* and *Zhouornis*. The jugal process of the maxilla is longer than the premaxillary process as in other bohaiornithids (Wang et al., 2010; Hu et al., 2011; O'Connor et al., 2013; Zhang et al., 2013; Figs. 3 and 8); the ventral margin of the maxilla appears to be slightly concave. An elongated oval fenestra is present on the dorsal part of the lateral surface of the base of the jugal process, ventral to the rostralmost part of the antorbital fossa. The margins of this opening are smooth, suggesting that the oval fenestra



Fig. 7 Photograph and line drawing of *Longisunguis kurochikini* gen. et sp. nov. holotype (IVPP V 17964)  
 Abbreviations: par. parapophyses 椎体横突; pot. posterior trochanter 后转子; other abbreviations follow Figs. 1 and 2



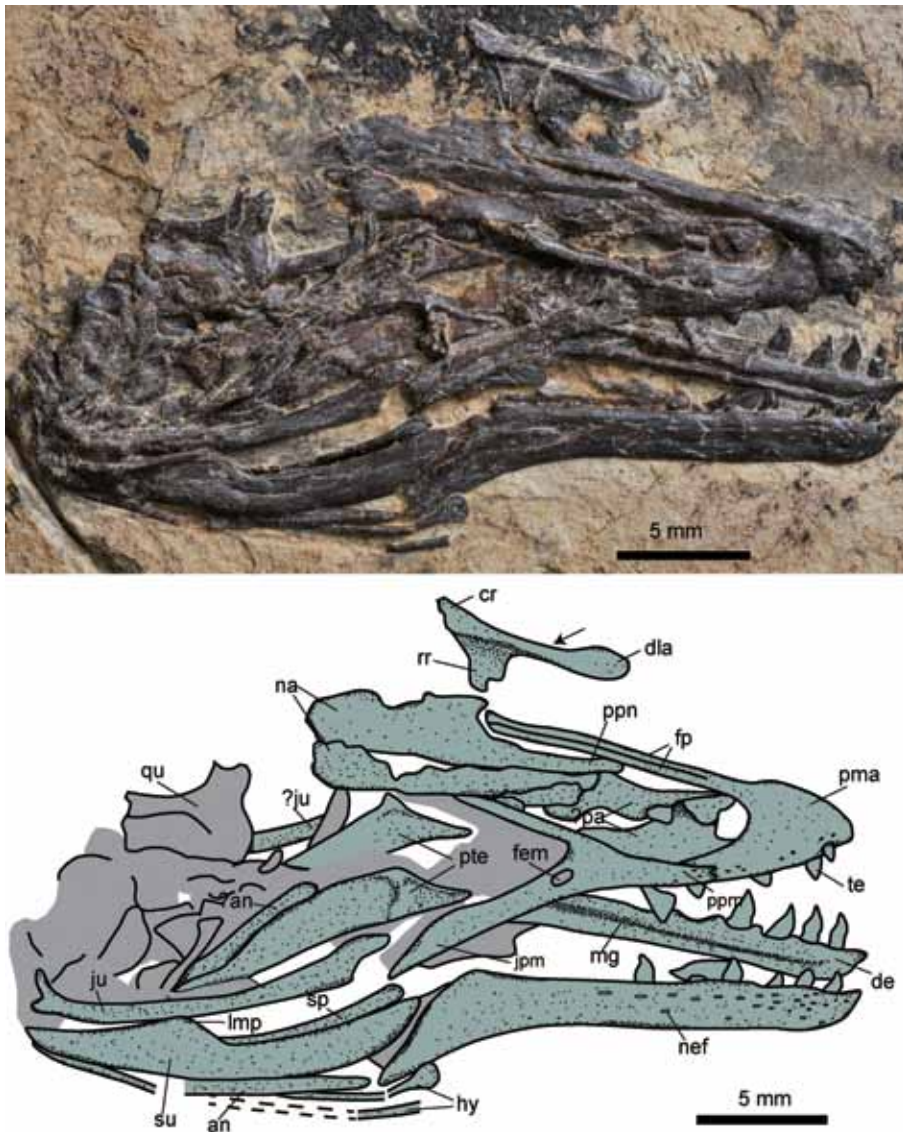


Fig. 8 Photograph and line drawing of the skull of the *Longusunguis kurochkini* gen. et sp. nov. holotype (IVPP V 17964)

Abbreviations: an. angular 隅骨; fem. fenestra of maxilla 上颌骨窗; jpm. jugal process of maxilla 上颌骨颧骨突; imp. lateral mandibular process 下颌外侧突; nef. nutrient foramina 滋养孔; pa. palatine 颧骨; ppn. premaxillary process of maxilla 上颌骨前颌骨突; ppn. premaxillary process of nasal 鼻骨前颌骨突; pte. pterygoid 翼骨; sp. splenial 夹板骨; qu, quadrate 方骨; other abbreviations follow Fig. 3. The black arrow indicates the elongated excavation on the caudal margin of the descending ramus of the lacrimal

is a natural feature rather than a result of over preservation. This opening is much larger than a nutrient foramen, and pierces the maxilla. A fenestra is present in the holotypes of *Pengornis* and *Zhouornis*, but in both taxa the fenestra perforates the recessed medial wall of the antorbital fossa as in *Archaeopteryx* (O'Connor and Chiappe, 2011; Zhang et al., 2013).

In *Pengornis* the fenestra is situated in the dorsorostral portion of the antorbital fossa (Zhou et al., 2008), whereas in *Zhouornis* the fenestra is present near the base of the dorsal process and is potentially homologous with the maxillary fenestra of *Archaeopteryx* and non-avian theropods (Zhang et al., 2013). Based on its position, the fenestra in *Longusunguis* is unlikely to share in this homology to the ancestral maxillary fenestra (Xu and Wu, 2001; Xu et al., 2004; Weishampel et al., 2004; Mayr et al., 2005; Norell et al., 2006; Godefroit et al., 2008). The maxilla is not perforated by a similar fenestra in *Shenqiornis* or *Bohaiornis*. Although the absence of a fenestra cannot be verified in *Sulcavis*, we infer that the fenestra probably represents an autapomorphy of *Longusunguis*. The distal end of the jugal process of the maxilla slopes ventrocaudally to articulate with the jugal, the rostral end of which forms a matching rostradorsally sloping articulation for the maxilla. As in *Shenqiornis*, the distal end of the jugal is forked, and the dorsal process is longer than the ventral process (Wang et al., 2010)(unforked in *Bohaiornis*, Li et al., in press). Several bones inferred to be palatal elements are preserved but obscured by crushing and overlap. Two rostrally tapered triangular bones preserved dorsal to the jugal are interpreted as the pterygoids.

The rostral ends of dentaries are unfused. Meckel's groove is visible, and deeply excavates the medial surface of the left dentary. As in *Parabohaiornis* and *Bohaiornis*, the groove does not extend to the rostral tip of the dentary. Six teeth are present in each lower jaw, located in the rostral half of the dentary as in *Parabohaiornis* and *Bohaiornis* (Li et al., in press; contra with Hu et al., 2011). *Longusunguis* accordingly has fewer dentary teeth than *Shenqiornis* and *Sulcavis* (Wang et al., 2010; O'Connor et al., 2013). As in other enantiornithines, the caudal end of the dentary slopes ventrally to form a ventrocaudal-rostradorsal articulation with the angular and surangular. The surangular is robust, shorter than the dentary, and three times the dorsoventral thickness of the angular. The surangular is convex ventrally, and also has a concave dorsal margin as in *Shenqiornis*. The dorsal margin is poorly preserved in other bohaiornithid birds, but straight in most enantiornithines (O'Connor and Chiappe, 2011). The caudal part of the dorsal margin forms a peak that may represent the lateral mandibular process or a primitive coronoid process, and similar structure is present in *Shenqiornis* and the referred specimen of *Bohaiornis* IVPP V 17963 (Li et al., in press). Caudal to the peak, the dorsal margin slants ventrally. The long and slender elements partially overlain by the right surangular may represent parts of the splenial, the angular and/or the hyoids. A single quadrate is preserved, and appears to bear only two mandibular condyles. We identify the quadrate as the left element, exposed in caudal view. Under this interpretation the medial condyle is larger than the lateral one and the caudal surface is excavated, as in *Zhouornis* and some other enantiornithines (e.g. *Rapaxavis*, O'Connor and Chiappe, 2011). It cannot be determined if a foramen pierced the caudal surface, as in some taxa including *Shenqiornis* and *Pengornis*.

**Axial skeleton** Six articulated cervicals are exposed in dorsal view (Fig. 7). Because the atlas and axis are not preserved, at least eight cervicals must have originally been present.

Some cervicals appear to be at least partially heterocoelous, as inferred from the exposed cranial articular surface of the first preserved cervical. The postzygapophyses are longer than the prezygapophyses, and well-developed epipophyses are present. The epipophyses are proximally located on the postzygapophyses and fails to extend caudally beyond their distal margins but become increasingly caudally located in the more caudally located cervicals. The spinous process is well developed on each of the four cranialmost cervicals. The seventh preserved vertebra is associated with a long rib, and thus is interpreted as the first thoracic vertebrae. The total number of thoracic vertebrae is eleven as in *Parabohaiornis* (unknown in other bohaiornithids). The cranialmost two thoracics are exposed in dorsal view, and the remainder in left lateral view. Only the sixth and seventh thoracics are disarticulated from the series. The neural spines are tall and expanded craniocaudally, contacting the preceding and following spines in the case of the third and fourth thoracic vertebrae. In each thoracic vertebra the postzygapophyses extend caudally beyond the vertebral body, and are longer than the prezygapophyses. As in other enantiornithines, the centrum bears a groove-like lateral excavation (Chiappe and Walker, 2002; O'Connor, 2009). The parapophyses are centrally positioned in craniocaudal dimension as in other enantiornithines (Chiappe and Walker, 2002; Zhou et al., 2008).

Although broken into five sections, the synsacrum is completely fused and is composed of seven to eight vertebrae, falling within the previously known range of bohaiornithid synsacral count. The dorsal surface bears a spinous crest that becomes dorsoventrally narrower and craniocaudally shorter distally. The second to last transverse process is robust, craniocaudally broad, and laterally directed. The last transverse process is more delicate and laterocaudally directed. The free caudal series is complete, containing seven vertebrae exposed in dorsal view. The spinous processes of the cranial five caudals are tall, but those of the last two are only weakly developed. The prezygapophyses are longer than the postzygapophyses, and project cranially beyond the centrum by a distance that is more than half the centrum length. Large plate-like chevrons articulate with the caudal vertebrae.

The pygostyle is longer than metatarsal III, whereas the opposite is true in other bohaiornithids. The pygostyle is exposed primarily in dorsal view, and is gently tapered caudally as in other bohaiornithids. As in other enantiornithines, the proximal end of the pygostyle is dorsally forked. It is unclear if paired laminar processes projecting ventrolaterally for most of the length of the pygostyle are also present as in most other enantiornithines (Chiappe and Walker, 2002; O'Connor, 2009). Proximally, the dorsal processes are short and extend for less than one seventh the length of the pygostyle, rather than being more elongate as in *Halimornis* (Chiappe et al., 2002).

**Thoracic girdle** The scapula is not curved along its length. The dorsal margin slopes ventrally while the ventral margin remains straight, forming a bluntly tapered distal tip, as in *Parabohaiornis* and *Shenqiornis* (Fig. 4). The acromion is expanded into a rectangular process as in *Enantiornis* and *Halimornis* (Chiappe et al., 2002; Walker and Dyke, 2009), but

differs from its counterparts in these taxa in being longer than the humeral articular facet of the scapula as in other bohaiornithids (unclear in *Sulcavis*). In contrast with the condition in *Bohaiornis*, *Parabohaiornis* and *Shenqiornis*, the acromion is distinctly deflected dorsally forming a large angle with the scapular shaft as in *Sulcavis* and most other enantiornithines, including *Elsornis*, *Eoalulavis*, *Gobipteryx* and *Protopteryx* (Elżanowski, 1981; Sanz et al., 1996; Zhang and Zhou, 2000; Chiappe et al., 2007b; O'Connor et al., 2013; Fig. 4).

The coracoids are exposed in dorsal view. Only the proximal end and the lateral part of the sternal end of the left coracoid are visible. Similarly, only the proximal end of the right coracoid is exposed. The acrocoracoid process is straight, and is aligned with the glenoid facet and the articular surface for the scapula, as in other enantiornithines (Chiappe and Walker, 2002). Unlike in some Late Cretaceous enantiornithines, there is no distinct acrocoracoid tubercle (Chiappe and Walker, 2002). The coracoid is strut-like, and the dorsal surface bears only a shallow depression similar to that seen in *Zhouornis* and some Jehol ornithuromorphs (e.g. *Yixianornis*), rather than a deep excavation as in Late Cretaceous enantiornithines (Chiappe and Walker, 2002). The coracoid differs from those of other bohaiornithids in that the distal half of the lateral margin is more convex, and in that the length of the convex part of the lateral margin is equal to the width of the sternal margin. The right coracoid shows that the sternal margin is weakly concave, as in other bohaiornithids. The sternal margin is proportionally wider than in *Sulcavis* and *Shenqiornis*, its width slightly exceeding half the length of the coracoid.

The furcula is largely covered by other elements, and only the omal halves of the rami and part of the hypocleidium are visible. The omal tips are bluntly expanded as in other bohaiornithids, but unlike in most other enantiornithines. A shallow depression, which may represent the articular facet for the coracoid, is developed on the lateral surface of the left omal tip. As in *Parabohaiornis* and *Zhouornis*, the hypocleidium extends well beyond the sternal margin of the coracoid and appears to be strongly mediolaterally compressed, giving the furcula a keeled appearance. The sternum is incomplete and the distal tip of the xiphoid is broken. The right and left costal margins are covered by other elements. The cranial margin is parabolic, lacking the well-defined craniolateral corner seen in *Zhouornis*. The exposed portions of the sternum are generally similar to their counter parts in *Parabohaiornis* and *Bohaiornis*.

**Thoracic limbs** Both humeri are exposed in caudal view (Fig. 7). The humeral head is concave in its central portion, but forms proximal convexities dorsally and ventrally, as in other enantiornithines (Chiappe and Walker, 2002). Caudally, the humeral head is strongly convex and separated from the ventral tubercle by the wide and shallow capital incision. As in *Parabohaiornis*, *Bohaiornis* and *Zhouornis*, the deltopectoral crest is weakly developed; it is less dorsoventrally wider than the shaft width and extends for only one third the humeral length. In contrast, the deltopectoral crest is well developed (as wide as the shaft) in *Sulcavis* (O'Connor et al., 2013). The distal margin of the humerus is angled less ventrally than in

*Bohaiornis*, *Parabohaiornis* and *Zhouornis*. No flexor process is evident. A shallow but broad depression appears to be present on the distalmost part of the caudal surface of the humerus, which is also visible in the right humerus of *Parabohaiornis* holotype, probably corresponding to a primitive humerotricipital sulcus. This sulcus was considered to be absent in enantiornithines by Chiappe and Walker (2002). Although a well-formed sulcus is indeed absent in some enantiornithines (e.g., *Zhouornis*), a depression like that in *Longusunguis* also occurs in *Kizylkumavis*, *Alexornis*, and the referred specimen of *Bohaiornis* V 17963 (Brodkorb, 1976; Nessonov, 1984; Li et al., in press), which suggest that humerotricipital sulcus is actually present in certain enantiornithines. No olecranon fossa or scapulotricipital groove is present.

The ulna is bowed proximally and straight distally, combining with the straight radius to define a large interosseous space with the radius, as is typical in enantiornithines and other Early Cretaceous birds. The ulna is robust, and approaches the dorsoventral width of the mid-shaft of the humerus. The olecranon process is weakly developed. Quill knobs are not visible even under magnification. As in other bohaiornithids, a groove like that present in Late Cretaceous enantiornithines is clearly visible on the caudodorsal surface of the radius (Chiappe and Walker, 2002), and this feature has also been reported in *Shenqiornis* (Wang et al., 2010).

The ulnare is heart-shaped with a shallow metacarpal incisure, as in *Parabohaiornis*, *Zhouornis* and *Sulcavis*, and differs from the equivalent bone in *Eocathayornis* and CAGS-IG-04-CM-023 in lacking distinct rami (Zhou, 2002; Harris et al., 2006). The radiale appears to be triangular and much smaller than the ulnare, as in *Bohaiornis*, *Sulcavis* and *Zhouornis*.

The semilunate carpal articulates exclusively with the proximal end of the major metacarpal, but the two bones are not fused together. This condition suggests that the specimen is a subadult, like *Parabohaiornis* holotype. As in other bohaiornithids, the alular metacarpal is nearly rectangular but is narrower proximally than distally (Wang et al., 2010; Zhang et al., 2013). The major and minor metacarpals are fused neither proximally nor distally. As is typical in enantiornithines, the minor metacarpal extends farther distally than the major metacarpal. The proximal phalanx of the major digit is robust and slightly wider than the major metacarpal, as in other bohaiornithids. A beveled caudodistal corner is present in this proximal phalanx. The second phalanx of the major digit is shorter and more slender than the preceding one, and is tapered distally. The claws of the alular and major digits are weakly curved, and that of the alular digit appears to be larger as in other bohaiornithids. The minor metacarpals appear to be wider than the major metacarpal, although this probably reflects the preserved orientation of these bones. The minor metacarpal is exposed in caudal rather than dorsal/ventral view, whereas the major metacarpal is in dorsal view. So the best interpretation is that the caudal surface of the minor metacarpal is wider than the dorsal surface of the major metacarpal. Only the proximal phalanx is preserved on the minor digit. The minor phalanx is robust, and the distal end is only slightly smaller than the proximal end. These features suggest that a second phalanx may have been present as in *Zhouornis* and *Shenqiornis* (Wang et al., 2010; O'Connor et al., 2013).

**Pelvic girdle** The pelvic elements are completely unfused around the margin of the acetabulum. The poorly preserved ilia reveal few anatomical details. The ischium is robust and about half the length of the pubis as in *Shenqiornis*. The ischium is proportionately longer in *Bohaiornis* and *Parabohaiornis*. A well developed dorsal process is present. In lateral view the ventral margin of the ischium is convex while the dorsal margin is straight. The ischium lacks the dorsal deflection seen in *Bohaiornis*, *Parabohaiornis* and *Sinornis* (Serenio et al., 2002). The pubic shaft is ventrally convex, and the distal end expands into a boot as in some other enantiornithines including other bohaiornithids (the distal end of the pubis is not preserved in *Sulcavis*). The distal portion of the right pubis is excavated medially by a shallow depression.

**Hindlimbs** The left femur is complete and preserved in lateral view. The proximal end is compressed severely, not preserving any discernible features. The right femur is missing the middle portion of the shaft, but the proximal and distal ends are well preserved in lateral and laterocaudal views, respectively. The femur is approximately 85% the length of the tibiotarsus. As in other bohaiornithids, the femur is straight. A well developed posterior trochanter is present near the proximal end of the lateral surface of the femur, representing a synapomorphy of Enantiornithes (Chiappe and Walker, 2002). The posterior trochanter is also visible in *Zhouornis*, but the relevant area is not exposed in other bohaiornithids. Distally, the lateral condyle and ectocondylar tubercle are continuous with a weakly developed fibular trochlea.

A true tibiotarsus is not formed—the proximal tarsals are fused to each other but not the tibia (Figs. 7 and 9), a condition we interpret as reflecting subadult ontogenetic status. Both tibiae are exposed in cranial view. Proximally, the tibia is similar to those of most other enantiornithines, including members of Bohaiornithidae, in lacking a cnemial crest (O'Connor et al., 2013; Zhang et al., 2013). The fibular crest is only visible in the case of the left tibia, and is preserved compressed against the dorsal surface of the bone. Distally, the dorsal surface of the tibia appears to be excavated by a shallow sulcus, although this could be an artifact of preservation. The distal condyles, formed by the proximal tarsals, are laterally displaced from the distal end of the tibia. The medial condyle is ball shaped in cranial view, and transversely wider than the lateral condyle. The lateral condyle is deeply excavated by a lateral epicondylar depression. An intercondylar incisure is absent, as in *Parabohaiornis* which also is likely absent from *Zhouornis* (see fig. 8 in Zhang et al., 2013), but a wide incisure is present in *Bohaiornis* and *Sulcavis* (Hu et al., 2011; O'Connor et al., 2013). The fibula is triangular with a broad proximal end in medial view. The shaft is sharply tapered distally and extremely reduced, terminating approximately one quarter of the way down the tibia. This makes the fibula proportionally shorter than in *Parabohaiornis*, *Sulcavis* and *Zhouornis*. The medial surface of the left fibula is visible, and is excavated by a medial fossa as in *Parabohaiornis* and *Bohaiornis*.

Metatarsals II, III and IV are displaced and are not preserved in natural articulation on either side, indicating that the proximal ends were not fused together (Fig. 9). A single distal tarsal is visible in the left ankle. As in the referred specimen of *Parabohaiornis* (V 18690),

the distal tarsal caps the proximal surface of metatarsals III and IV, barely contacting metatarsal II.

The metatarsals are similar in their relative lengths to those of other bohaiornithids (Wang et al., 2010; Hu et al., 2011; O'Connor et al., 2013; Zhang et al., 2013; Li et al., in press): metatarsal III is the longest, closely followed by metatarsal IV; metatarsal II is the shortest, and terminates proximal to the level of the proximal end of the metatarsal III trochlea. The left metatarsal II is exposed in plantar view, and a sulcus extends along the proximal fourth of the plantar surface of the shaft. Distal to the sulcus, the plantar surface bears a medial plantar crest. The metatarsal II trochlea is weakly ginglymoid as in *Parabohaiornis* and *Bohaiornis*. The right and left metatarsal III are exposed in plantar and medioplantar views, respectively. The plantar surface is flat and conspicuously less convex than that of metatarsal II, although this may be exaggerated by preservation. Distally, the lateral and medial rims of the trochlea are equal in proximal extension. However, the medial rim of the trochlea is more prominent in the plantar direction than the lateral rim as in avisaurid enantiornithines such as *Avisaurus*, *Soroavisaurus* and *Neuquenornis* from Upper Cretaceous of Argentina (Chiappe, 1992, 1993; Chiappe and Calvo, 1994). This is also apparently present in the metatarsal II trochlea of *Longusunguis*, but this condition is unknown in other bohaiornithids. Metatarsal I is 'P' shaped in plantar view with a medially deflected distal end, as in other bohaiornithids and many other enantiornithines.

The pedal digits are morphologically similar to those of other bohaiornithids (Fig. 7). Digit II is more robust than the other digits. The proximal three phalanges of digit IV are notably shorter than the penultimate phalanx, whereas the proximal phalanx is nearly as long as the fourth in *Sulcavis* and *Zhouornis*. The third phalanx of digit III is longer than the second phalanx of the same digit.

**Plumage** The feathers preserved close to the skull and pectoral girdle are short and curved, lacking distinct rachises, and we interpret them as body coverts. Five pennaceous feathers, which could be either rectrices or leg feathers, are clearly recognizable adjacent to the pygostyle and the right tibia (Fig. 9), and additional feathers may be present. The recognizable feathers are all on the right side of the pygostyle and are preserved parallel to



Fig. 9 The right leg of *Longusunguis kurochkini* gen. et sp. nov. holotype (IVPP V 17964). The white arrows indicate five pennaceous feathers, which we interpret as leg feathers (see text)



the bone, although the distal ends of three of the feathers curve towards the pygostyle. In some enantiornithines from the Jehol Biota, the tail coverts radiate from the pygostyle and form a large acute angle with the shaft (Zhang and Zhou, 2004; Zheng et al., 2007; Zheng et al., 2013b); besides, two long rectrices are preserved in the *Bohaiornis* holotype, which are close to the humeral length and substantially longer than these feathers in *Longusunguis* (Hu et al., 2011), leading us to suggest that the feathers preserved in the present specimen are more likely to be leg feathers, than rectrices. This interpretation is consistent with the fact that these feathers, when traced proximally, end adjacent to the surface of the tibial shaft. If they are indeed leg feathers, this specimen would provide additional evidence that leg feathers are widely distributed among Early Cretaceous enantiornithines (Zheng et al., 2013b).

## 5 Phylogenetic analysis of the Bohaiornithidae

We performed a phylogenetic analysis on a revised version of the data matrix of O'Connor and Zhou (2013). Descriptions of 11 characters from this dataset were modified or expanded to include additional character states. A few characters with ambiguous scorings (see Appendix 1) were changed based on direct observations of relevant holotype specimens (e.g., those of *Archaeorynchus*, *Schizooura* and *Hongshanornis*) and recent literatures (Wang et al., 2010; Gao et al., 2012; Zhou et al., 2013). In addition, 17 new characters were added to the analysis. Scorings for *Parabohaiornis*, *Longusunguis* and *Bohaiornis* were based on the holotypes and, when necessary, on referred specimens. *Zhouornis* was scored based on an epoxy resin cast of the holotype. Two additional enantiornithines *Qiliania* and V 18631, were added to the matrix and were scored based on Ji et al. (2011) and direct examination of the specimen, respectively. The modified data matrix consists of 56 taxa and 262 morphological characters, 33 of which are ordered (see Appendices 1 and 2 for character description and scorings).

The phylogenetic analysis was run using TNT [version 1.1] (Goloboff et al., 2008). The matrix was analyzed using an unconstrained traditional heuristic search starting with Wagner trees with following options: 1000 replicates of random stepwise addition (branch swapping: tree-bisection-reconnection, TBR), holding ten trees at each step. All characters were given equal weight, and branches with minimum branch lengths of zero were collapsed to create polytomies. Bootstrap and absolute Bremer values were calculated as indexes of clade support. Bootstrap analysis was conducted with 1000 replicates with the same setting as in the most parsimonious trees (MPTs) search.

The cladistic analysis recovered eight MPTs. In the strict consensus of these trees, *Bohaiornis*, *Parabohaiornis*, *Longusunguis*, *Shenqiornis*, *Zhouornis* and *Sulcavis* form a family, Bohaiornithidae, which occupies a derived position within Enantiornithes (Fig. 10). The new cladogram is largely consistent in topology with those generated in previous studies (Zhou and Zhang, 2005; O'Connor et al., 2009; Zhou et al., 2009). However, the large polytomies recovered in some previous analyses (O'Connor and Zhou, 2013) are better



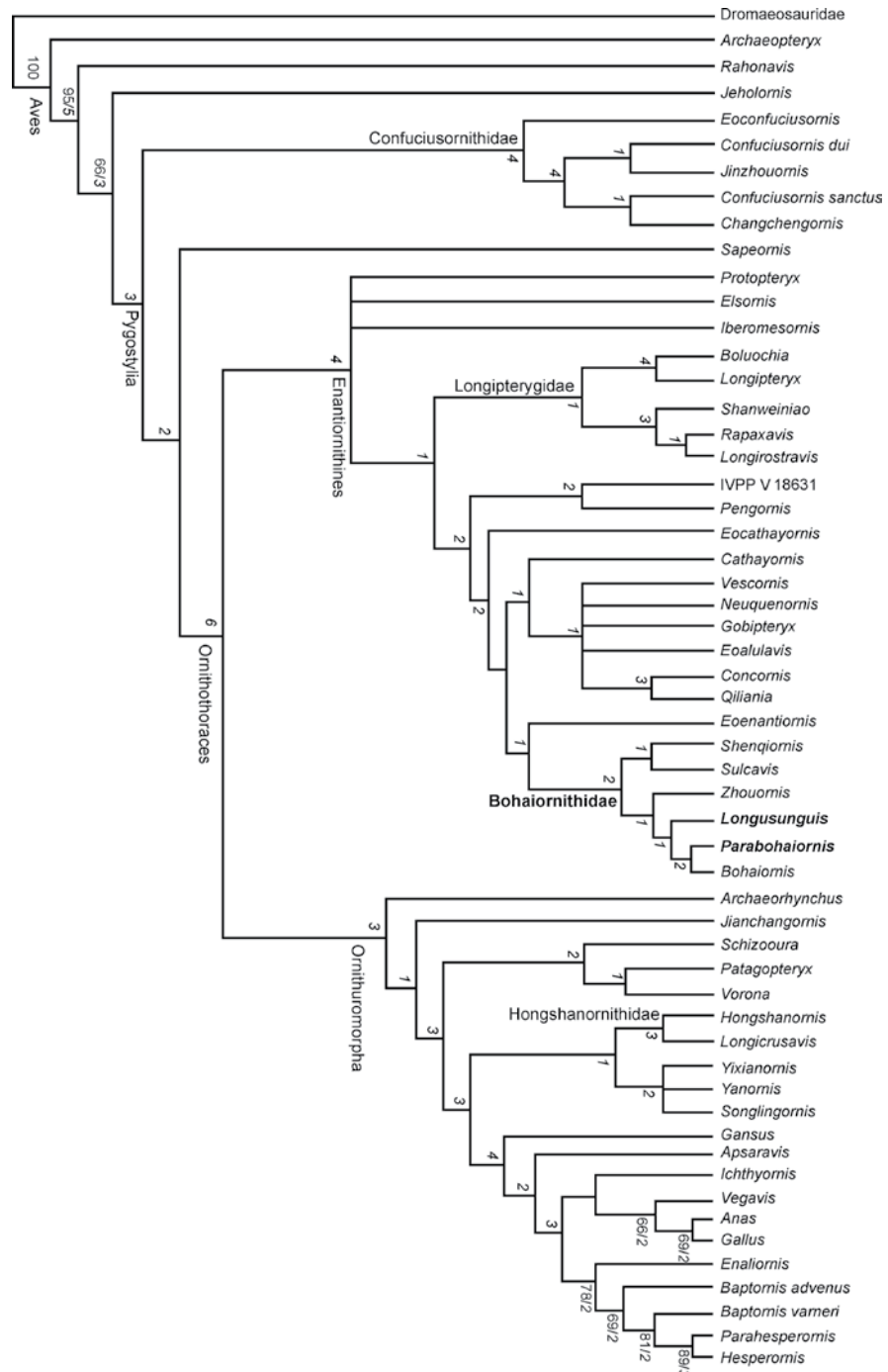


Fig. 10 The strict consensus of the eight most parsimonious trees recovered in our analysis (Length = 993, CI = 0.367, RI = 0.676) indicates that *Parabohaiornis martini* gen. et sp. nov. (IVPP V 18691) and *Longusunguis kurochkini* gen. et sp. nov. (IVPP V 17964) are closely related to *Bohaiornis*, *Sulcavis*, *Zhouornis* and *Shenqiornis*, with all six taxa making up the new family, Bohaiornithidae  
 Bootstrap values (where greater than 50%) and absolute Bremer support values are indicated in regular and bold italic type, respectively, under the nodes to which they apply

resolved here, which suggests the new characters and additional taxa improved resolution. *Sapeornis* is placed in a more derived position than Confuciusornithidae, forming the outgroup to Ornithothoraces (Gao et al., 2008; O'Connor and Zhou, 2013) in contrast to some previous studies that recovered Confuciusornithidae in a more derived position (Clarke et al., 2006; Zhou et al., 2008; Xu et al., 2011).

Within Enantiornithes, *Propteryx*, *Elsornis* and *Iberomesornis* were recovered in a basal polytomy. Longipterygidae (*sensu* O'Connor et al., 2011c) formed the outgroup to the remaining enantiornithines. An elongate rostrum and other shared morphological features suggest close affinities between *Longipteryx*, *Boluochia*, *Shanweinia*, *Rapaxavis* and *Longirostravis* (O'Connor et al., 2009, 2011b, c). Previous studies proposed these five taxa form a family, called Longipterygidae (O'Connor et al., 2011b, c). However, the existence of this family has never been fully confirmed in phylogenetic studies (O'Connor and Zhou, 2013; O'Connor et al., 2013). In our analysis Longipterygidae was recovered as a monophyletic group consisting of two smaller clades: *Longipteryx* + *Boluochia*, and *Shanweinia* + (*Rapaxavis* + *Longirostravis*). Longipterygidae is supported by three synapomorphies: ischium more than two thirds as long as pubis (character 188:1); pubic pedicel of ilium very laterally compressed and hook-like (character 195:1); and acromion process much longer than humeral articular facet (character 249:2). Within Longipterygidae, a sister-taxon relationship between *Longipteryx* and *Boluochia* was previously inferred by O'Connor and Zhou (2013), and is supported by four synapomorphies: maxillary process of premaxilla at least subequal in length to facial portion of maxilla (character 2:1); metatarsal III intermediate to metatarsal II and IV in distal extension (character 235:3); lateral trabecula of sternum is caudolaterally directed (character 246:1); metatarsal IV surpasses the distal end of metatarsal III (character 255:2); and ratio of tibiotarsus length to tarsometatarsus length smaller than 1.6 (character 257:2). *Shanweinia* falls outside the *Rapaxavis* + *Longirostravis* clade, and the clade formed by all three taxa is supported by five synapomorphies: costal surface of scapula without prominent longitudinal furrow (character 103:0); ungual phalanx of major digit absent (character 172:1); manus shorter than humerus (character 176:2); metatarsal II terminates at level of proximal end of trochlea for metatarsal IV (character 236:2); and penultimate phalanx of each pedal digit longer than preceding phalanges (character 258:1).

*Eocathayornis* and a clade comprising *Pengornis* and V 18631 were recovered as the successively distant outgroups to the remaining enantiornithines, which were grouped into two clades. Within one clade, *Cathayornis* was recovered as the outgroup to a polytomy of *Vescornis*, *Neuquenornis*, *Gobipteryx*, *Eoalulavis* and a *Qiliania* + *Concornis* clade. *Eoenantiornis* was recovered as the outgroup to Bohaiornithidae. The bohaiornithid family is supported by three synapomorphies: scapula with convex dorsal margin and straight ventral margins (character 96:1); intermetacarpal space terminating distal to end of alular metacarpal (character 165:1); and lateral trabecula of sternum distinctly caudolaterally directed (character 246:1). Within Bohaiornithidae, *Sulcavis* and *Shenqiornis* formed a clade supported by one

synapomorphy (hand as long as humerus, character 176:1), and *Longusunguis* and *Zhouornis* form successively distant outgroups to the derived *Bohaiornis* + *Parabohaiornis* clade. The clade comprising *Bohaiornis*, *Parabohaiornis* and *Longusunguis* is supported by two synapomorphies: prezygapophyses of distal caudal vertebrae exceed length of centrum by more than 25% (character 72:0), and distal end of pubis expanded into simple pubic foot (character 198:0). The derived *Bohaiornis* + *Parabohaiornis* clade is supported by three synapomorphies: intermembral index [(combined length of humerus and ulna)/ (combined length of femur and tibiotarsus)] greater than 1.1 (character 177:3); deltopectoral crest recedes gently into humeral shaft (character 253:1); and tibiotarsus twice as long as tarsometatarsus (character 257:0).

Our analysis resolved most relationships within Ornithuromorpha although the three members of Songlingornithidae (*Yanornis*, *Yixianornis* and *Songlingornis*) formed a trichotomy. Previous studies placed *Yanornis* in a basal position relative to the other two taxa (Clarke et al., 2006; Zhou et al., 2010). *Archaeorhynchus* emerged as the most basal ornithuromorph in our analysis, as in previous studies (Zhou et al., 2008; O'Connor and Zhou, 2013).

## 6 Discussion

*Parabohaiornis* and *Longusunguis* share several synapomorphies of Enantiornithes, e.g., 'Y' shaped furcula, minor metacarpal extending farther distally than major metacarpal, reduced metatarsal IV (Chiappe and Walker, 2002), indicating they are members of this diverse clade. This conclusion is corroborated by the result of our cladistic analysis. In addition, several unique morphological features shared by *Bohaiornis*, *Sulcavis*, *Shenqiornis*, *Zhouornis*, *Parabohaiornis* and *Longusunguis* distinguish them from other enantiornithines: the rostrum is robust; the teeth are large and subconical with sharply tapered and slightly caudally recurved tips (crown base width: *Parabohaiornis*, c. 0.74–0.89 mm; *Longusunguis*, c. 0.73–0.89 mm; *Bohaiornis*, c. 0.72–0.98 mm; *Zhouornis*, 0.72–0.90 mm; *Shenqiornis*, c. 0.84–0.91 mm; *Sulcavis*, c. 0.79–0.86 mm), whereas the teeth of many other Mesozoic birds are either simple and peg-like (e.g., *Archaeopteryx*, *Sapeornis*, *EoEnantiornis*), small and blunt teeth (*Pengornis*, in which the crown base width is only c. 0.58–0.61 mm, although *Pengornis* is much larger than the largest known bohaiornithid specimen by 26%), or strongly curved (e.g., *Longipteryx*); omal tips of furcula bearing blunt expansions, rather than being tapered as in most other enantiornithines (e.g., *Eoenantiornis*, *Protopteryx*, *Pengornis*, *Concornis*, *Iberomesornis*); pygostyle tapers gently toward distal end without distinct constriction seen in many other enantiornithines (e.g., *Rapaxavis*, *Shanweiniao*, *Halimornis*); tarsometatarsus is short and robust; and pedal unguis are distinctly elongated, and the unguis in the digit III approaches half the length of tarsometatarsus, proportionally much longer than that of all known Mesozoic birds (Table 2). Bohaiornithids also have a distinctive sternal morphology. The lateral trabeculae of the sternum are strongly caudolaterally directed, a feature that among basal birds is only known in certain enantiornithines including *Elsornis*, *Vescornis* and *Longipteryx*. The

shape of the distal expansions of the lateral trabeculae varies among enantiornithines from simple and fan-shape in *Longipteryx* to complex and branched in *Longirostravis* (O'Connor, 2009). In *Bohaiornis*, *Zhouornis* and *Parabohaiornis* (also likely in *Shenqiornis*, inferred from impression of lateral trabeculae; unknown in *Sulcavis* and *Longusunguis*) the distal end is expanded into an asymmetrical triangle, with an acute medial angle. The impression that bohaiornithids have several important morphological features in common was supported by our cladistic analysis, which recovered a monophyletic clade consisting of *Shenqiornis*, *Bohaiornis*, *Sulcavis*, *Zhouornis*, *Parabohaiornis* and *Longusunguis*. Therefore, we erect a new family, Bohaiornithidae, for these six species with robust rostra and tasometatarsi. The characters that distinguish bohaiornithid taxa from other enantiornithines (morphological features of teeth, acromion process, lateral trabecula of sternum, omal tips of furcula, robust rostrum and tasometatarsi, and the pygostyle) do not appear strongly susceptible to ontogenetic variation. The available specimens of *Parabohaiornis* and *Longusunguis* are probably subadults as opposed to early juveniles, and are therefore unlikely to show large ontogenetic differences from the adult condition (see following section). Therefore, we feel justified in the erection of new genera for IVPP V 17964 and V 18691.

In the past two decades, approximately 27 enantiornithine taxa have been named from the Jehol Biota (Zhou and Zhang, 2006a; O'Connor and Dyke, 2010). Until now, the Longipterygidae represented the most diverse widely recognized family of Early Cretaceous enantiornithines and the only family supported by phylogenetic analysis (O'Connor et al., 2009). Given the new results of the cladistic analysis herein, Longipterygidae includes five genera: *Longipteryx*, *Longirostravis*, *Boluochia*, *Shanweinia* and *Rapaxavis* (O'Connor et al., 2011c). Li et al. (2010) named a new putative longipterygid, *Camptodontus yangi*, based on an incomplete skeleton; regardless of the fact the generic name is already taken by a genus of beetle, the features proposed to be diagnostic for this taxon are actually widely shared among enantiornithines (e.g., carina restricted to caudal part of sternum, cranial cervicals heterocoelous, ulna longer than humerus). Furthermore, the preserved morphological features of the holotype of "*Camptodontus yangi*" (large teeth strongly curved caudally, lateral trabecula of sternum slightly laterally directed with simple distal expansion) correspond closely to those of *Longipteryx*; therefore, the holotype of this putative species is referable to *Longipteryx*. Zhou et al. (1992) proposed the existence of a family, Cathayornithidae, which contains three genera, *Cathayornis*, *Sinornis* and *Eocathayornis* added later by Zhou and Hou (2002) and Zhou (2002), although *Cathayornis* and *Sinornis* have been considered synonymous by some authors (Serenó et al., 2002; Cau and Arduini, 2008). A total of four species have been assigned to *Cathayornis* (Zhou et al., 1992; Hou, 1997; Hou et al., 2002; Li et al., 2008), bringing the total number of "cathayornithids" to six species. The validity of the various species assigned to *Cathayornis* has never been conclusively established (Serenó et al., 2002; Zhou and Hou, 2002; O'Connor and Dyke, 2010) although some diagnostic characters have been shown to be invalid (O'Connor, 2009). Furthermore, neither Cathayornithidae

Zhou et al., 1992 nor Cathayornithiformes Zhou et al., 1992 has ever been supported by a phylogenetic analysis (O'Connor and Zhou, 2013; O'Connor et al., 2013; Fig. 10). The recognition of Bohaiornithidae greatly increases our understanding of enantiornithine higher level relationships. Currently six taxa are known, making Bohaiornithidae even more diverse than Longipterygidae (five taxa).

Bohaiornithids show much less variation in size and morphology than longipterygids: tooth morphology varies greatly in longipterygids but is very consistent in bohaiornithids; longipterygids span a large size range (e.g., the humerus of *Longipteryx* holotype is nearly twice as long as that of *Shanweinia* holotype), whereas all bohaiornithids are similar in size; and distal expansions of the lateral trabecula of sternum occupy the entire morphological spectrum (e.g., unbranched, forked, moose horn) in longipterygids, but are essentially uniform in bohaiornithids. Therefore, it seems that bohaiornithids diversified in a much more morphologically conservative way than did longipterygids. *Bohaiornis*, *Parabohaiornis*, *Sulcavis* and *Longsunguis* are probably all from the Jiufotang Formation near Lamadong Town (although the provenance of *Zhouornis* is not clear, Zhang et al., 2013), making bohaiornithids more narrowly distributed than longipterygids (O'Connor et al., 2011c). Bohaiornithids are generally similar to one another in size and tooth morphology, possibly indicating that they occupied a narrower range of morphologies and presumably ecotypes than do longipterygids. *Shenqiornis* was collected from the Qiaotou Formation in northern Hebei (nearly 300 km from Lamadong Town), which is equivalent to the Dawangzhangzi Bed of the Yixian Formation (Jin et al., 2008). This indicates the Bohaiornithidae persisted at least five million years, as long as Longipterygidae (125–120 Ma, He et al., 2004; Yang et al., 2007). The older stratigraphic position of *Shenqiornis* is consistent with the basal position of this taxon within Bohaiornithidae in the cladistic analysis presented here. Furthermore, the real temporal ranges of Bohaiornithidae and Longipterygidae could be considerably longer, giving the fact that their derived position within Enantiornithes.

## 7 Ecological and ontogenetic characteristics of Bohaiornithidae

Many studies (e.g. Leisler et al., 1989; Landmann and Winding, 1993; Hopson, 2001; Green et al., 2009) have confirmed the existence in birds of a correlation between foot morphology and ecology. Therefore, the distinctive robust foot and hyperelongated pedal claws of bohaiornithids warrant ecological discussion. Compared to other Jehol birds, the third pedal digit ungual of bohaiornithids is proportionally long with respect to the tarsometatarsus (Table 2). The tarsometatarsus is approximately as long relative to the femur and tibiotarsus as in other Jehol birds, and therefore the high ratio of pedal ungual length to tarsometatarsus length reflects elongation of the former rather than shortening of the latter (Table 2).

We added bohaiornithids to the data set of Hopson (2001), which included a large number of modern and fossil arboreal and terrestrial birds. When the expanded data set is used

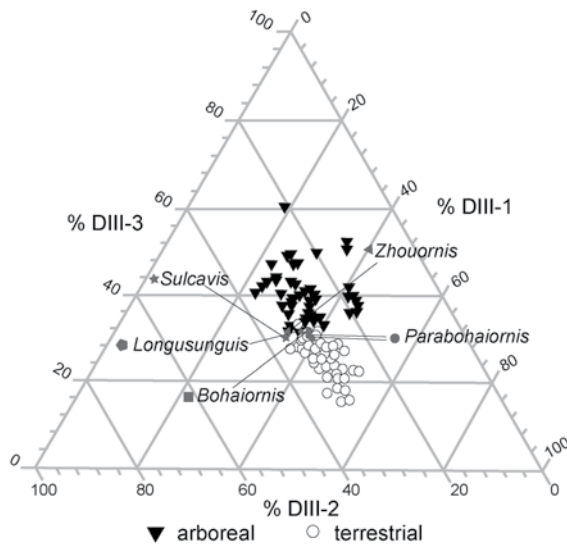


Fig. 11 Ternary diagram of phalangeal proportions of digit III of *Parabohaiornis martini* gen. et sp. nov. (holotype IVPP V 18691 and a referred specimen V 18690), *Longusunguis kurochkini* gen. et sp. nov. (holotype IVPP V 17964), *Bohaiornis*, *Zhouornis*, *Sulcavis* holotypes and many other fossil and extant birds, based on data from Hopson (2001) and Morschhauser et al. (2009)

to construct a ternary plot of phalangeal proportions within digit III, arboreal birds normally have an elongated penultimate phalanx in digit III. All bohaiornithids fall close to the border between the interpenetrating clusters formed by extant terrestrial and arboreal birds (Fig. 11), as do the basal birds *Archaeopteryx* and *Confuciusornis* (Hopson, 2001). However, the strongly curved claws of bohaiornithids preclude these birds from being terrestrial, as the claws of modern terrestrial birds generally show a low degree of curvature (Pike and Maitland, 2004). Bohaiornithids are generally similar in their claw curvature to extant raptors, as well as to tree-trunk climbing and arboreal birds (Pike and Maitland, 2004). Tree-trunk climbing lifestyle seems improbable

for bohaiornithids given that extant avian trunk climbers normally have specialised hindlimb proportions (Richardson, 1942; Zelenkov and Dzerzhinsky, 2006; see also measurements in Hopson, 2001). It is also unlikely that bohaiornithids were raptorial like extant accipitrines, given that bohaiornithids possess a short tarsometatarsus and rather gracile digits III and IV. Modern raptors normally have a long tarsometatarsus, which is advantageous for seizing and subsequently transporting the prey; however, short tarsometarsus are also present in many other raptors, e.g., *Chondrohierax*, *Pernis* and *Leptodon*. Among raptors, only ospreys (Pandionidae) have hindlimb proportions similar to that of bohaiornithids (see Hopson, 2001). Ospreys and other piscivorous raptors are further characterized by very long claws (Fowler et al., 2009), although their claws are also more curved than in those of other accipitrines (Pike and Maitland, 2004) or of bohaiornithids. Therefore, a piscivorous diet remains plausible for bohaiornithids despite poor support from other lines of evidence such as the tooth morphology, which in bohaiornithids seems more adapted to durophagy than is the case in other enantiornithines (O'Connor and Chiappe, 2011; O'Connor et al., 2013).

Judging from the strong recurvature of their claws (especially when the horny sheaths are taken into account), it is likely that bohaiornithids were arboreal, although the details of their ecology remain unknown. Previous studies suggested an arboreal lifestyle for all Jehol enantiornithines (Sereno et al., 2002; Zhou, 2004; Zhang et al., 2004; Zhou and Zhang, 2005; Morschhauser et al., 2009). As in many other enantiornithines, the feet of bohaiornithids

have features that indicate they lacked the degree of perching specialization seen in modern arboreal birds: the hallux is relatively short; metatarsal I articulates on the medial rather than plantar surface of metatarsal II, and the distal half of metatarsal I is not strongly twisted in the plantar direction, all of which indicate that the hallux is not fully opposable. Enantiornithes were probably bad perchers compared with extant perching birds and many of them possessed only a partially reversed hallux (Kurochkin and Bogdanovich, 2008), but fully opposable hallux seen in certain taxa, like *Sinornis* and *Concornis*, implies relatively advanced perching ability (Serenó et al., 2002). However, this observation alone does not weigh strongly against the possibility that bohaiornithids and other enantiornithines were arboreal. In the absence of competition with highly specialized perchers, especially Jehol ornithuromorphs all inferred to have been terrestrial, enantiornithines were likely successful arboreal taxa, although one fossil evidence suggested that *Microraptor* preyed on small enantiornithines (O'Connor et al., 2011a).

The Bohaiornithidae represents a new and diverse enantiornithine family, currently including six genera represented by eight known specimens. These specimens vary in size and skeletal maturity, and provide an opportunity to address some ontogenetic questions. The *Zhouornis* holotype and the referred specimen of *Bohaiornis* (V 17963), are the largest individuals, and are interpreted as adults based on the presence in both of fused compound bones, e.g., carpometacarpus, tibiotarsus and tarsometatarsus. The absence of a fused carpometacarpus, tibiotarsus and tarsometatarsus indicates that the available specimens of *Shenqiornis*, *Parabohaiornis* and *Longusunguis* are not adult; the fused tarsometatarsus in *Sulcavis* suggests the specimen was somewhat more mature, although still not adult, at the time of death. However, the bone surface of all the known individuals of *Shenqiornis*, *Parabohaiornis* and *Longusunguis* lacks evident foramina or striations of the type characteristically seen in juvenile or younger individuals (Tumarkin-Deratzian et al., 2006; Chiappe et al., 2007a). The non-adult specimens also display complete or near-complete synsacral fusion and are only slightly smaller than the adult, further suggesting that they are relatively mature and had reached the subadults stage by the time of death. The long bones of the holotype of *Bohaiornis* are only roughly 10% smaller than their equivalents in the referred specimen (V 17963), but the carpometacarpus, tibiotarsus and tarsometatarsus of the holotype remain unfused. This implies that fusion of the compound bones happened relatively late in ontogeny, when an individual was already close to full body size (Cambra-Moo et al., 2006); histological study indicated that the *Zhouornis* holotype individual had reduced its rate of bone deposition and experienced at least one annual period of arrested growth (marked by one line of arrested growth) by the time of death (Zhang et al., 2013). Based on histological comparisons to Late Cretaceous enantiornithines, the *Zhouornis* holotype was inferred to have reached sexual maturity (growth rate decreased) but not skeletal maturity (lacking outer circumferential layer or external fundamental system, Chinsamy, 2005; Woodward et al., 2011; Zhang et al., 2013); the fused compound bones in this specimen suggest that fusion is

complete before the individual reach adult size, and possibly in other enantiornithines as well. Compound bone fusion begins during early embryonic stages in some modern birds (Blom and Lilja, 2004; Maxwell, 2008). However, few studies have investigated the timing of compound bone fusion in Mesozoic birds, a critical ontogenetic parameter; so far, the pattern of fusion has been studied extensively only in the sternum (Zheng et al., 2012). In the holotype of *Sulcavis* the tarsometatarsus is fused whereas the carpometacarpus and tibiotarsus remain unfused, indicating that the tarsometatarsus fused earlier than other compound bones in this taxon. In contrast with the situation for enantiornithines, non-adult Mesozoic ornithuromorphs are poorly known, except in *Archaeorhynchus*. The tibiotarsus and tarsometatarsus are unfused in all known specimens of this genus, which have accordingly been interpreted as subadults (Zhou and Zhang, 2006b; Zhou et al., 2013). Considering that their synsacum and pygostyle are incompletely fused, all the specimens of *Archaeorhynchus* appear to be less mature than the known sub-adult bohaiornithid specimens. However, no adult *Archaeorhynchus* is available, and therefore it is impossible to determine at what point during ontogeny these compound bones fused in basal ornithuromorphs, making comparison with the contemporaneous enantiornithines impossible at present.

**Acknowledgments** We thank LI Yutong and LI Dahan for preparing the fossils, and ZHANG Jie for photograph. We also thank WANG Xiaolin, LI Zhiheng and LIU Di for discussion. We are grateful to the reviewers Corwin Sullivan and LI Zhiheng for their constructive comments on this manuscript. This research was supported by the National Basic Research Program of China (973 Program, 2012CB821906), and the National Natural Science Foundation of China (41172020).

**Appendices 1 and 2** can be found at the website of Vertebrata Palasiatica (<http://english.ivpp.cas.cn/sp/Palasiatica/vp.list/>), in Vol. 52, No.1.

## 中国早白垩世反鸟类一新科 (Bohaiornithidae fam. nov.)

王 敏<sup>1,2</sup> 周忠和<sup>1</sup> 邹晶梅<sup>1</sup> Nikita V. ZELENKOV<sup>3</sup>

(1 中国科学院古脊椎动物与古人类研究所, 脊椎动物演化与人类起源重点实验室 北京 100044)

(2 中国科学院大学 北京 100049)

(3 俄罗斯科学院Borissiak古生物研究所 莫斯科 117997)

**摘要:** 依据3件近乎完整的骨骼化石, 记述了辽宁建昌早白垩世湖相地层九佛堂组反鸟类的两个新属种: 马氏副渤海鸟(*Parabohaiornis martini* gen. et sp. nov.)和库氏长爪鸟(*Longsunguis kurochkini* gen. et sp. nov.)。这两个新属种与此前报道的渤海鸟(*Bohaiornis*)、神七鸟(*Shenqiornis*)、齿槽鸟(*Sulcavis*)和周鸟(*Zhouornis*)具有一些独特的形态特征, 包括



吻端粗壮、牙齿粗大并近似锥形、叉骨上升支的末端明显膨大、胸骨的后外侧突向外侧强烈偏转、跗跖骨粗短、第三脚趾具有很长的爪子。对包含有大量中生代鸟类和形态特征的矩阵进行了系统发育分析,其结果显示这两个新属种与上述的这些反鸟构成了一个单系类群,基于此建立了一个新科——渤海鸟科。渤海鸟科包括6个属,代表了目前已知的反鸟类中多样性最丰富的一个类群,进一步增加了我们对于反鸟类高阶分类单元之间亲缘关系的认识。渤海鸟科强壮的吻端和脚爪表明其占据了不同于其他早白垩世反鸟的生态位。

关键词: 早白垩世, 热河生物群, 反鸟类, *Bohaiornis*, *Shenqiornis*, *Sulcavis*, *Zhouornis*

中图法分类号: Q915.865 文献标识码: A 文章编号: 1000-3118(2014)01-0031-46

## References

- Barsbold R, Osmólska H, 1999. The skull of *Velociraptor* (theropoda) from the Late Cretaceous of Mongolia. *Acta Palaeontol*, 44: 189–219
- Baumel J J, Witmer L M, 1993. Osteologia. In: Baumel J J, King A S, Breazile J E et al. eds. *Handbook of Avian Anatomy: Nomina Anatomica Avium*. Publ Nuttall Ornithol Club, 23: 45–132
- Bellairs A D A, Jenkin C R, 1960. The skeleton of birds. In: Marshall J A ed. *Biology and comparative physiology of birds*. Vol. 1. New York: Academic Press. 241–300
- Blom J, Lilja C, 2004. A comparative study of growth, skeletal development and eggshell composition in some species of birds. *J Zool*, 262: 361–369
- Brodkorb P, 1976. Discovery of a Cretaceous bird, apparently ancestral to the orders Coraciiformes and Piciformes (Aves: Carinatae). *Smithson Contrib Paleobiol*, 27: 67–73
- Cambra-Moo O, Buscalioni Á D, Cubo J et al., 2006. Histological observations of enantiornithine bone (*Saurischia*, Aves) from the Lower Cretaceous of Las Hoyas (Spain). *C R Palevol*, 5: 685–691
- Cau A, Arduini P, 2008. *Enantiophoenix electrophyla* gen. et sp. nov. (Aves, Enantiornithes) from the Upper Cretaceous (Cenomanian) of Lebanon and its phylogenetic relationship. *Atti Soc Ital Sci Nat Mus Civ Stor Nat Milano*, 149: 293–324
- Chang M M, Chen P J, Wang Y Q et al., 2001. *The Jehol Biota*. Shanghai: Shanghai Science and Technology Publishers. 1–208
- Chiappe L M, 1992. Enantiornithine (aves) tarsometatarsi and the avian affinities of the Late Cretaceous Avisauridae. *J Vert Paleont*, 12: 344–350
- Chiappe L M, 1993. Enantiornithine (Aves) tarsometatarsi from the Cretaceous Lecho Formation of northwest Argentina. *Am Mus Novit*, 3083: 1–27
- Chiappe L M, 1996. Late Cretaceous birds of southern South America: anatomy and systematics of Enantiornithes and *Patagopteryx deferrariisi*. *Münchner Geowiss Abh*, 30: 203–244
- Chiappe L M, 2007. *Glorified Dinosaurs: the Origin and Early Evolution of Birds*. Hoboken, New Jersey: John Wiley & Sons. 1–263
- Chiappe L M, Calvo J O, 1994. *Neuquenornis volans*, a new Late Cretaceous bird (Enantiornithes: Avisauridae) from Patagonia, Argentina. *J Vert Paleont*, 14: 230–246
- Chiappe L M, Ji S A, Ji Q, 2007a. Juvenile birds from the Early Cretaceous of China: implications for enantiornithine ontogeny. *Am Mus Novit*, 3594: 1–46

- Chiappe L M, Ji S A, Ji Q et al., 1999. Anatomy and systematics of the Confuciusornithidae (Theropoda: Aves) from the Late Mesozoic of northeastern China. *Bull Am Mus Nat Hist*, 242: 1–89
- Chiappe L M, Lamb J P, Erickson P G P, 2002. New enantiornithine bird from the marine Upper Cretaceous of Alabama. *J Vert Paleont*, 22: 170–174
- Chiappe L M, Suzuki S, Dyke G J et al., 2007b. A new enantiornithine bird from the Late Cretaceous of the Gobi desert. *J Syst Palaeont*, 5: 193–208
- Chiappe L M, Walker C A, 2002. Skeletal morphology and systematics of the Cretaceous Euenantiornithes (Ornithothoraces: Enantiornithes). In: Chiappe L M, Witmer L eds. *Mesozoic Birds: Above the Heads of Dinosaurs*. Berkeley: University of California Press. 240–267
- Chinsamy A, 2005. *The Microstructure of Dinosaur Bone*. Baltimore: Johns Hopkins University Press. 1–195
- Clarke J A, Zhou Z H, Zhang F C, 2006. Insight into the evolution of avian flight from a new clade of Early Cretaceous ornithurines from China and the morphology of *Yixianornis grabaui*. *J Anat*, 208: 287–308
- Codd J R, 2010. Uncinate processes in birds: morphology, physiology and function. *Comp Biochem Phys Part A: Mol Integr Phys*, 156(3): 303–308
- Codd J R, Manning P L, Norell M A et al., 2008. Avian-like breathing mechanics in maniraptoran dinosaurs. *Proc R Soc Ser B*, 275: 157–161
- Elzanowski A, 1981. Embryonic bird skeletons from the Late Cretaceous of Mongolia. *Palaeont Pol*, 42: 147–176
- Feduccia A, 1993. Evidence from claw geometry indicating arboreal habits of *Archaeopteryx*. *Science*, 259: 790–793
- Fowler D W, Freedman E A, Scannella J B, 2009. Predatory functional morphology in raptors: interdigital variation in talon size is related to prey restraint and immobilisation technique. *PloS ONE*, 4: e7999
- Gao C L, Chiappe L M, Meng Q J et al., 2008. A new basal lineage of Early Cretaceous birds from China and its implications on the evolution of the avian tail. *Palaeontology*, 51: 775–791
- Gao C L, Chiappe L M, Zhang F J et al., 2012. A subadult specimen of the Early Cretaceous bird *Sapeornis chaoyangensis* and a taxonomic reassessment of sapeornithids. *J Vert Paleont*, 32: 1103–1112
- Godefroit P, Currie P J, Li H et al., 2008. A new species of *Velociraptor* (Dinosauria: Dromaeosauridae) from the Upper Cretaceous of northern China. *J Vert Paleont*, 28: 432–438
- Goloboff P A, Farris J S, Nixon K C, 2008. TNT, a free program for phylogenetic analysis. *Cladistics*, 24: 774–786
- Green R E, Barnes K N, de Brooke M, 2009. How the longspur won its spurs: a study of claw and toe length in ground-dwelling passerine birds. *J Zool*, 277: 126–133
- Harris J D, Lamanna M C, You H L et al., 2006. A second enantiornithine (Aves: Ornithothoraces) wing from the Early Cretaceous Xiagou Formation near Changma, Gansu Province, People's Republic of China. *Can J Earth Sci*, 43: 547–554
- He H Y, Wang X L, Zhou Z H et al., 2004. Timing of the Jiufotang Formation (Jehol Group) in Liaoning, northeastern China, and its implications. *Geophys Res Lett*, 31: L12605, doi:10.1029/2004GL019790
- Hopson J A, 2001. Ecomorphy of avian and nonavian theropod phalangeal proportions: implications for the arboreal versus terrestrial origin of bird flight. In: Gauthier J, Gall L F eds. *New Perspectives on the Origin and Evolution of Birds: Proceedings of the International Symposium in Honor of John H. Ostrom*. New Haven: Peabody Museum of Natural History, Yale University. 211–235
- Hou L H, 1997. *Mesozoic Birds of China*. Nantou: Feng-Huang-Ku Bird Park of Taiwan Provincial Government. 1–228
- Hou L H, Zhou Z H, Zhang F C et al., 2002. *Mesozoic Birds from Western Liaoning in China*. Shenyang: Liaoning Science

- and Technology Publishing House. 1–120
- Howard H, 1929. The avifauna of Emeryville shell mound. *Univ Calif Publ Zool*, 32: 301–394
- Hu D Y, Li L, Hou L H et al., 2011. A new enantiornithine bird from the Lower Cretaceous of western Liaoning, China. *J Vert Paleont*, 31: 154–161
- Ji S A, Atterholt J, O'Connor J K et al., 2011. A new, three-dimensionally preserved enantiornithine bird (Aves: Ornithothoraces) from Gansu Province, north-western China. *Zool J Linn Soc*, 162: 201–219
- Jin F, Zhang F C, Li Z H et al., 2008. On the horizon of *Protopteryx* and the early vertebrate fossil assemblages of the Jehol Biota. *Chin Sci Bull*, 53: 2820–2827
- Kurochkin E N, 1996. A new enantiornithid of the Mongolian Late Cretaceous, and a general appraisal of the infraclass Enantiornithes (Aves). *Paleont Inst Russ Acad Sci, Spec Issue*: 1–50
- Kurochkin E N, Bogdanovich I A, 2008. On the origin of avian flight: compromise and system approach. *Biol Bull*, 35: 1–11
- Landmann A, Winding N, 1993. Nich segregation in high-altitude Himalayan chats (Aves, Turdidae): does morphology match ecology? *Oecologia*, 95: 506–519
- Leisler B, Ley H W, Winkler H, 1989. Habitat, behavior and morphology of *Acrocephalus warblers*: an integrated analysis. *Ornis Scand*, 20: 181–186
- Li J J, Li Z H, Zhang Y G et al., 2008. A new species of *Cathayornis* from Lower Cretaceous of Inner Mongolia, China and its stratigraphic significance. *Acta Geol Sin*, 82: 1115–1123
- Li L, Gong E P, Zhang L D et al., 2010. A new enantiornithine bird (Aves) from the Early Cretaceous of Liaoning, China. *Acta Palaeont Sin*, 49(4): 524–531
- Li Z H, Zhou Z H, Wang M et al. (in press). A new specimen of large-bodied basal enantiornithine *Bohaiornis* from the Early Cretaceous of China and the inference of feeding ecology in Mesozoic birds. *J Paleont*
- Maxwell E E, 2008. Comparative embryonic development of the skeleton of the domestic turkey (*Meleagris gallopavo*) and other galliform birds. *Zoology*, 111: 242–257
- Mayr G, Pohl B, Peters D S, 2005. A well-preserved *Archaeopteryx* specimen with theropod features. *Science*, 310: 1483–1486
- Morschhauser E M, Varricchio D J, Gao C L et al., 2009. Anatomy of the Early Cretaceous bird *Rapaxavis pani*, a new species from Liaoning Province, China. *J Vert Paleont*, 29: 545–554
- Nessov L A, 1984. Upper Cretaceous pterosaurs and birds from Central Asia. *Paleont J*, 18: 38–49
- Norell M A, Clark J M, Turner A H et al., 2006. A new dromaeosaurid theropod from Ukhaa Tolgod (Ömnögov, Mongolia). *Am Mus Novit*, 3545: 1–51
- O'Connor J K, 2009. A systematic review of Enantiornithes (Aves: Ornithothoraces). Ph.D. dissertation. Los Angeles: University of Southern California. 1–600
- O'Connor J K, 2012. A revised look at *Liaoningornis longidigitrus* (Aves). *Vert Palasiat*, 50(1): 25–37
- O'Connor J K, Chiappe L M, 2011. A revision of enantiornithine (Aves: Ornithothoraces) skull morphology. *J Syst Palaeont*, 9: 135–157
- O'Connor J K, Chiappe L M, Gao C L et al., 2011c. Anatomy of the Early Cretaceous enantiornithine bird *Rapaxavis pani*. *Acta Palaeont Pol*, 56: 463–475
- O'Connor J K, Dyke G, 2010. A reassessment of *Sinornis santensis* and *Cathayornis yandica* (Aves: Enantiornithes). *Rec Aust Mus*, 62: 7–20
- O'Connor J K, Wang X R, Chiappe L M et al., 2009. Phylogenetic support for a specialized clade of Cretaceous

- enantiornithine birds with information from a new species. *J Vert Paleont*, 29: 188–204
- O'Connor J K, Zhang Y G, Chiappe L M et al., 2013. A new enantiornithine from the Yixian Formation with the first recognized avian enamel specialization. *J Vert Paleont*, 33: 1–12
- O'Connor J K, Zhou Z H, 2013. A redescription of *Chaoyangia beishanensis* (Aves) and a comprehensive phylogeny of Mesozoic birds. *J Syst Palaeont*, 11: 889–906
- O'Connor J K, Zhou Z H, Xu X, 2011a. Additional specimen of *Microraptor* provides unique evidence of dinosaurs preying on birds. *Proc Nat Acad Sci*, 108: 19662–19665
- O'Connor J K, Zhou Z H, Zhang F C, 2011b. A reappraisal of *Boluochia zhengi* (Aves: Enantiornithes) and a discussion of intraclade diversity in the Jehol avifauna, China. *J Syst Palaeont*, 9: 51–63
- Pike A V L, Maitland D P, 2004. Scaling of bird claws. *J Zool*, 262: 73–81
- Richardson F, 1942. Adaptive modifications for tree-trunk foraging in birds. *Univ Calif Publ Zool*, 46: 317–368
- Sanz J L, Chiappe L M, Pérez-Moreno B P et al., 1996. An Early Cretaceous bird from Spain and its implications for the evolution of avian flight. *Nature*, 382: 442–445
- Sanz J L, Pérez-Moreno B P, Chiappe L M et al., 2002. The birds from the Lower Cretaceous of Las Hoyas (Province of Cuenca, Spain). In: Chiappe L M, Witmer L eds. *Mesozoic Birds: Above the Heads of Dinosaurs*. Berkeley: University of California Press. 209–229
- Sereno P C, Rao C G, Li J J, 2002. *Sinornis santensis* (Aves: Enantiornithes) from the Early Cretaceous of northeastern China. In: Chiappe L M, Witmer L eds. *Mesozoic Birds: Above the Heads of Dinosaurs*. Berkeley: University of California Press. 184–208
- Tumarkin-Deratzian A R, Vann D R, Dodson P, 2006. Bone surface texture as an ontogenetic indicator in long bones of the Canada goose *Branta canadensis* (Anseriformes: Anatidae). *Zool J Linn Soc*, 148: 133–168
- Walker C A, Dyke G J, 2009. Euenantiornithine birds from the Late Cretaceous of El Brete (Argentina). *Irish J Earth Sci*, 27: 15–62
- Wang M, Zhou Z H, Xu G H (in press a). The first enantiornithine bird from the Upper Cretaceous of China. *J Vert Paleont*, 34(1)
- Wang M, O'Connor J K, Zhou Z H (in press b). A new robust enantiornithine bird from the Lower Cretaceous of China with scansorial adaptations. *J Vert Paleont*, 34(2)
- Wang X R, O'Connor J K, Zhao B et al., 2010. New species of enantiornithes (Aves: Ornithothoraces) from the Qiaotou Formation in northern Hebei, China. *Acta Geol Sin*, 84: 247–256
- Weishampel D B, Dodson P, Osmolska H, 2004. *Dinosauria*. 2nd ed. Berkeley: University of California Press. 1–833
- Woodward H N, Horner J, Farlow J O, 2011. Osteohistological evidence for determinate growth in the American alligator. *J Herpetol*, 45(3): 339–342
- Xu X, Norell M A, Kuang X W et al., 2004. Basal tyrannosauroids from China and evidence for protofeathers in tyrannosauroids. *Nature*, 431: 680–684
- Xu X, Wu X C, 2001. Cranial morphology of *Sinornithosaurus millenii* Xu et al. 1999 (Dinosauria: Theropoda: Dromaeosauridae) from the Yixian Formation of Liaoning, China. *Can J Earth Sci*, 38: 1739–1752
- Xu X, You H L, Du K et al., 2011. An *Archaeopteryx*-like theropod from China and the origin of Avialae. *Nature*, 475: 465–470
- Xu X, Zheng X T, You H L, 2009. A new feather type in a nonavian theropod and the early evolution of feathers. *Proc Nat Acad Sci*, 106: 832–834
- Xu X, Zheng X T, You H L, 2010. Exceptional dinosaur fossils show ontogenetic development of early feathers. *Nature*,

- 464: 1338–1341
- Xu X, Zhou Z H, Prum R O, 2001. Branched integumentary structures in *Sinornithosaurus* and the origin of feathers. *Nature*, 410: 200–204
- Yang W, Li S G, Jiang B Y, 2007. New evidence for Cretaceous age of the feathered dinosaurs of Liaoning: zircon U-Pb SHRIMP dating of the Yixian Formation in Sihetun, Northeast China. *Cretaceous Res*, 28(2): 177–182
- Zelenkov N V, Dzerzhinsky F Y, 2006. The hind limb structure and climbing in woodpeckers. *Zool Zh*, 85: 395–410
- Zhang F C, Ericson P G P, Zhou Z H, 2004. Description of a new enantiornithine bird from the Early Cretaceous of Hebei, northern China. *Can J Earth Sci*, 41: 1097–1107
- Zhang F C, Zhou Z H, 2000. A primitive enantiornithine bird and the origin of feathers. *Science*, 290: 1955–1959
- Zhang F C, Zhou Z H, 2004. Leg feathers in an Early Cretaceous bird. *Nature*, 431: 925
- Zhang F C, Zhou Z H, Hou L H et al., 2001. Early diversification of birds: evidence from a new opposite bird. *Chin Sci Bull*, 46: 945–949
- Zhang Z H, Chiappe L M, Han G et al., 2013. A large bird from the Early Cretaceous of China: new information on the skull of Enantiornithines. *J Vert Paleont*, 33: 1176–1189
- Zheng X T, O'Connor J K, Huchzermeyer F et al., 2013a. Preservation of ovarian follicles reveals early evolution of avian reproductive behaviour. *Nature*, 495: 507–511
- Zheng X T, Wang X L, O'Connor J K et al., 2012. Insight into the early evolution of the avian sternum from juvenile enantiornithines. *Nat Commun*, 3: 1116
- Zheng X T, Zhang Z H, Hou L H, 2007. A new enantiornithine bird with four long rectrices from the Early Cretaceous of northern Hebei, China. *Acta Geol Sin*, 81: 703–708
- Zheng X T, Zhou Z H, Wang X L et al., 2013b. Hind wings in basal birds and the evolution of leg feathers. *Science*, 339: 1309–1312
- Zhou S, Zhou Z H, O'Connor J K, 2013. Anatomy of the basal ornithuromorph bird *Archaeorhynchus spathula* from the Early Cretaceous of Liaoning, China. *J Vert Paleont*, 33: 141–152
- Zhou Z H, 2002. A new and primitive enantiornithine bird from the Early Cretaceous of China. *Vert PalAsiat*, 22: 49–57
- Zhou Z H, 2004. The origin and early evolution of birds: discoveries, disputes, and perspectives from fossil evidence. *Naturwissenschaften*, 91: 455–471
- Zhou Z H, 2006. Evolutionary radiation of the Jehol Biota: chronological and ecological perspectives. *Geol J*, 41: 377–393
- Zhou Z H, Barrett P M, Hilton J, 2003. An exceptionally preserved Lower Cretaceous ecosystem. *Nature*, 421: 807–814
- Zhou Z H, Chiappe L M, Zhang F C, 2005. Anatomy of the Early Cretaceous bird *Eoenantiornis buhleri* (Aves: Enantiornithes) from China. *Can J Earth Sci*, 42: 1331–1338
- Zhou Z H, Clarke J, Zhang F C, 2008. Insight into diversity, body size and morphological evolution from the largest Early Cretaceous enantiornithine bird. *J Anat*, 212: 565–577
- Zhou Z H, Hou L H, 2002. The discovery and study of Mesozoic birds in China. In: Chiappe L M, Witmer L eds. *Mesozoic Birds: Above the Heads of Dinosaurs*. Berkeley: University of California Press. 160–183
- Zhou Z H, Jin F, Zhang J Y, 1992. Preliminary report on a Mesozoic bird from Liaoning, China. *Chin Sci Bull*, 37: 1365–1368
- Zhou Z H, Li Z H, Zhang F C, 2010. A new Lower Cretaceous bird from China and tooth reduction in early avian evolution. *Proc R Soc Ser B*, 277: 219–227

- Zhou Z H, Zhang F C, 2003a. *Jeholornis* compared to *Archaeopteryx*, with a new understanding of the earliest avian evolution. *Naturwissenschaften*, 90: 220–225
- Zhou Z H, Zhang F C, 2003b. Anatomy of the primitive bird *Sapeornis chaoyangensis* from the Early Cretaceous of Liaoning, China. *Can J Earth Sci*, 40: 731–747
- Zhou Z H, Zhang F C, 2005. Discovery of an ornithurine bird and its implication for Early Cretaceous avian radiation. *Proc Nat Acad Sci*, 102: 18998–19002
- Zhou Z H, Zhang F C, 2006a. Mesozoic birds of China — a synoptic review. *Vert Palasiat*, 44: 74–98
- Zhou Z H, Zhang F C, 2006b. A beaked basal ornithurine bird (Aves, Ornithurae) from the Lower Cretaceous of China. *Zool Scr*, 35: 363–373
- Zhou Z H, Zhang F C, Li Z H, 2009. A new basal ornithurine bird (*Jianchangornis microdonta* gen. et sp. nov.) from the Lower Cretaceous of China. *Vert Palasiat*, 47: 299–310



## 北美古脊椎动物学会第73届年会在美国洛杉矶举行

北美古脊椎动物学会(Society of Vertebrate Paleontology, SVP)第73届年会于2013年10月30~11月2日在美国加利福尼亚州洛杉矶市顺利召开,来自世界各地的1000余名古脊椎动物学者参加了此次盛会。北美古脊椎动物年会由北美古脊椎动物学会主办,是全球最大的古脊椎动物专题会议,旨在交流与推动全球古脊椎动物学的研究进展。

此次年会由洛杉矶自然历史博物馆(Natural History Museum of Los Angeles County)主办,纪念该博物馆百年华诞,同时也是全球最富盛名的史前奇迹之一——位于洛杉矶奇迹大道上的拉布雷亚沥青坑(La Brea Tar Pits)发掘100周年。会议设4场专题讨论会:“拉布雷亚及更多:沥青生物群的古生物学研究”,“个体发育改变一切:恐龙生长的古生物学意义”,“两极的演化:高纬度地区脊椎动物化石多样性与古生态学”和“脊椎动物演化的节拍:地质年代学在化石测年方面的进展”。本次会议还组织了15场常规报告和4场板报展览,内容覆盖古脊椎动物学、地层学以及相关领域的最新研究进展。近年来,利用高精度CT扫描和虚拟3D技术对化石进行探查、重建和复原已逐渐成为古脊椎动物学研究的常规手段,本次会议也针对这一趋势开展了系列专题讲座。

中国科学院古脊椎动物与古人类研究所的朱敏、尤海鲁、白滨、卢静、Corwin Sullivan、Jingmai O'Connor、Brian Choo、Thomas Stidham等人参加了此次会议。他们通过会议报告或展板的形式介绍了中国古脊椎动物学界在早期硬骨鱼类起源、肉鳍鱼类脑颅演化、恐龙个体发育、鸟类起源与演化、下孔亚纲动物功能形态学以及早始新世哺乳动物头后骨骼形态学等方面取得的相关进展。

下届年会将于2014年11月5~8日在德国柏林举行。

(卢静)